Molecular Pharmacology Fast Forward. Published on November 25, 2014 as DOI: 10.1124/mol.114.095422
This article has not been copyedited and formatted. The final version may differ from this version.



# Engineered hyperphosphorylation of the $\beta_2$-adrenoceptor prolongs arrestin-3 binding and induces arrestin internalization

Diana Zindel, Adrian J. Butcher, Suleiman Al-Sabah, Peter Lanzerstorfer, Julian Weghuber, Andrew B. Tobin, Moritz Bünemann, Cornelius Krasel

Institut für Pharmakologie und Klinische Pharmazie, Philipps-Universität Marburg, 35043 Marburg, Germany

Affiliations:

Institut für Pharmakologie und Klinische Pharmazie, Philipps-Universität Marburg, 35043 Marburg, Germany: DZ, MB, CK

MRC Toxicology Unit, University of Leicester, Leicester, LE2 2RG, United Kingdom: AJB, ABT

Dept. of Pharmacology and Toxicology, Kuwait University, Kuwait: SAS

University of Applied Sciences Upper Austria, Wels, Austria: PL, JW

Molecular Pharmacology Fast Forward. Published on November 25, 2014 as DOI: 10.1124/mol.114.095422
This article has not been copyedited and formatted. The final version may differ from this version.



Running title: Dynamics of arrestin-3-receptor complexes

Corresponding author: Cornelius Krasel, Institut für Pharmakologie und Klinische Pharmazie, Karl-von-Frisch-Str. 1, 35043 Marburg, Germany; email: cornelius.krasel@staff.uni-marburg.de; phone: +49 6421 28 25705; fax: +49 6421 28 25720

Number of text pages: 33
Number of tables: 1
Number of figures: 10
Number of supplemental figures: 2

Number of references: 36
Number of words:
Abstract: 218
Introduction: 574
Discussion: 1276



Abbreviations: arr-3: arrestin-3; β2AR: β2-adrenoceptor; CFP: cyan fluorescent protein; FRAP: fluorescence recovery after photobleaching; FRET: fluorescence resonance energy transfer; GPCR: G-protein-coupled receptor; GRK: G-protein-coupled receptor kinase; YFP: yellow fluorescent protein

Molecular Pharmacology Fast Forward. Published on November 25, 2014 as DOI: 10.1124/mol.114.095422
This article has not been copyedited and formatted. The final version may differ from this version.



## Abstract

G-protein-coupled-receptor phosphorylation plays a major role in receptor desensitization and arrestin binding. It is, however, unclear how distinct receptor phosphorylation patterns may influence arrestin binding and subsequent trafficking. Here we engineer phosphorylation sites into the C-terminal tail of the β2-adrenoceptor (β2AR) and demonstrate that this mutant, termed β2AR$^{SSS}$, showed increased isoprenaline-stimulated phosphorylation and differences in arrestin-3 affinity and trafficking. By measuring arrestin-3 recruitment and the stability of arrestin-3-receptor complexes in real time using fluorescence resonance energy transfer and fluorescence recovery after photobleaching, we demonstrate that arrestin-3 dissociated quickly, and almost completely from the β2AR, whereas the interaction with β2AR$^{SSS}$ was two- to four-fold prolonged. In contrast, arrestin-3 interaction with a β2-adrenoceptor fused to the carboxyl-terminal tail of the vasopressin type 2 receptor was nearly irreversible. Further analysis of arrestin-3 localization revealed that by engineering phosphorylation sites into β2-adrenoceptor the receptor showed prolonged interaction with arrestin-3 and colocalization with arrestin in endosomes following internalization. This is in contrast to the wild-type receptor that interacts transiently with arrestin-3 at the plasma membrane. Furthermore β2AR$^{SSS}$ internalized more efficiently than the wild-type receptor, whereas recycling was very similar for both receptors. Thus we show how the interaction between arrestins and receptors can be increased with minimal receptor modification, and that relatively modest increases in receptor-arrestin affinity are sufficient to alter arrestin trafficking.

Molecular Pharmacology Fast Forward. Published on November 25, 2014 as DOI: 10.1124/mol.114.095422
This article has not been copyedited and formatted. The final version may differ from this version.



## Introduction

Arrestins are a small family of four homologous proteins that have evolved as multifunctional scaffolding and adaptor proteins in G-protein-coupled-receptor (GPCR) signaling and trafficking. High-affinity arrestin interaction with GPCRs is mediated by a two-step process that involves receptor activation and phosphorylation in a synergistic fashion. Phosphorylation of agonist activated receptors is catalyzed by G-protein-coupled receptor kinases (GRKs), of which seven different isoforms have been identified (Pitcher *et al.*, 1998). Almost all GPCRs are phosphorylated by one or more of the seven GRKs which are, besides arrestin binding, receptor desensitization and uncoupling of G-proteins, considered to regulate cell type specific receptor signaling (Tobin et al., 2008). For rhodopsin it has been shown that the extent of arrestin receptor interaction varies in a systematic manner with the number of residues that are phosphorylated (Vishnivetskiy *et al.*, 2007). In the β2AR the three serine residues S355, S356 and S364 have a pivotal role in GRK-mediated phosphorylation and desensitization (Seibold *et al.*, 2000; Vaughan *et al.*, 2006) as well as arrestin binding (Krasel et al., 2008). The recently developed "bar code" hypothesis postulates that site-specific phosphorylation of GPCRs may regulate specific signaling outcomes (Tobin et al., 2008). Studies that support this hypothesis have been published recently for the β2-adrenoceptor (Nobles et al., 2011), muscarinic acetylcholine receptor $M_3$ (Butcher et al., 2011), CCR7 (Zidar et al., 2009) and the vasopressin type 2 receptor (V2R) (Ren et al., 2005). On the other hand, for the activity of rhodopsin it has been shown that receptor activity depends solely on the number but not on the identity of phosphorylation sites (Doan *et al.*, 2006). Based on the apparent stability of arrestin-receptor complexes, GPCRs have been divided into two classes, A and B (Oakley et al., 2000). Class A receptors such as the β2-adrenoceptor, μ-opiod receptor or endothelin type A receptor recruit preferentially arrestin-3 and show a transient arrestin interaction primarily at the plasma membrane. In contrast, class B receptors, e.g. the V2R or the angiotensin II type 1A receptor, bind both arrestin2 and arrestin-3 with similar high affinities and colocalize with them on endosomes (Oakley et al., 2000). The swapping of the C-termini of β2-adrenoceptor and V2R was found to reverse the trafficking pattern and signaling properties of arrestin (Oakley et al., 2001; Oakley et al., 2000; Tohgo et al., 2003). Recently a similar phenomenon was described for the switch of the C-termini of the NK1R and $PAR_2$ (Pal et al., 2013). In both cases, clusters of Ser and Thr residues

Molecular Pharmacology Fast Forward. Published on November 25, 2014 as DOI: 10.1124/mol.114.095422
This article has not been copyedited and formatted. The final version may differ from this version.



localized approximately 20-30 amino acids away from the membrane were proposed to be the major binding sites for arrestins. It was suggested that clusters of phosphorylated residues would increase the affinity of arrestin for the receptor. However, these findings were obtained by switching the entire C-termini of different receptors. It is known that receptor C-termini possess additional functions in addition to arrestin binding. For example, the C-terminus of the β2AR provides binding sites for adaptor proteins like Grb2 (Karoor et al., 1998) and PDZ-binding proteins like NHERF (Hall et al., 1998) which promotes rapid recycling of the receptor after agonist-induced internalization (Cao *et al.*, 1999). In this study we investigate whether the insertion of an additional cluster of serines into the C-terminus of the β2AR 20 amino acids away from the membrane, as previously proposed by Oakley et al. (2001), can indeed enhance arrestin binding affinity to the receptor and alter arrestin trafficking without affecting other properties such as receptor recycling.

Molecular Pharmacology Fast Forward. Published on November 25, 2014 as DOI: 10.1124/mol.114.095422
This article has not been copyedited and formatted. The final version may differ from this version.



## Material and methods

Unless otherwise stated, all biochemical and reagents were from Sigma (Taufkirchen, Germany).

*DNA constructs and transient expression in HEK 293T cells or stable expression in HEK 293 cells*

The following constructs have been described elsewhere: the β2V2R in which the C-terminal tail has been replaced with the V2R-tail (Oakley et al., 1999), the phosphorylation-deficient β2AR ($\beta2AR^{pd}$) lacking all putative phosphorylation sites except for the PKA phospho-sites (Bouvier et al., 1988), arrestin-3-CFP (Krasel *et al.*, 2005) , GRK2 (Krasel et al., 2001), Gβ1-Cer (Frank et al., 2005), $G\alpha_s$ (Hein et al., 2006) and $G\gamma_2$ (Lutz et al., 2005). Mutations were inserted into the β2AR by site-directed mutagenesis. The $\beta2AR^{SSS}$ was generated by replacing G-361, E-362 and Q-363 of the YFP-labeled or the unlabeled, N-terminally Flag-tagged receptor with serine residues. The $\beta2AR^{AAA}$ was constructed by replacing G-361, E-362 and Q-363 of the YFP-labeled or the unlabeled receptor with alanine residues. β2AR 2S was generated by reintroducing Ser 355/356 into the $\beta2AR^{pd}$ construct. β2AR 3S was constructed by replacing G-361, E-362 and Q-363 of the β2AR pd construct with serine residues, and the β2AR 5S construct was produced by applying both steps successively. β2AR SSS distal was generated by replacing N-398, I-399 and D-400 with serines. The amino acid sequences encoded by the different receptor constructs are shown in figure 1. Receptor constructs that were used for the FRAP assay were N-terminally tagged with YFP (Dorsch *et al.*, 2009). mCherry-tagged EEA1 was constructed by replacing the GFP in EEA1-GFP (a gift from Nicholas Holliday and Simon Davies, University of Nottingham, UK) with mCherry. All cDNAs were cloned into the pcDNA3 expression vector (Invitrogen, Darmstadt, Germany) and verified by sequencing. HEK 293T cells were maintained in DMEM supplemented with 10% fetal calf serum (FCS), penicillin (50 µg/ml) and streptomycin (50 µg/ml). Stable and transient transfections were performed using Effectene (Quiagen, Hilden, Germany) following the manufacturer´s protocol.

Molecular Pharmacology Fast Forward. Published on November 25, 2014 as DOI: 10.1124/mol.114.095422
This article has not been copyedited and formatted. The final version may differ from this version.



*Receptor expression levels*

HEK293 cells stably expressing Flag-β2AR, Flag-β2AR$^{SSS}$ or β2AR$^{AAA}$ were generated by standard procedures using G418 (600 µg/ml) selection. To determine receptor expression levels in membranes from these cells, confluent grown cells were washed in ice-cold PBS and detached with buffer composed of 50 mM NaCl, 20 mM $NaH_2PO_4$, 3 mM $MgCl_2$, 1 mM EDTA, pH 7.4 containing protease inhibitor cocktail from Roche (1 tablet per 10 ml). Membranes were pelleted by centrifugation at 14.000 rpm for 1 hr at 4°C. The pellet was washed in 100 mM NaCl, 20 mM Tris pH 7.4, resuspended in the same buffer and subsequently sonified. Membrane receptor binding was measured using saturating concentrations of [$^3$H]dihydroalprenolol. Nonspecific binding was measured in the presence of 100 µM alprenolol. Binding was performed overnight at 4°C and bound and unbound ligand were separated on GF/C glass fiber filters (Whatman, Dassel, Germany) by vacuum filtration. Filters were washed four times with 4 ml ice-cold buffer (50 mM Tris HCl, 120 mM NaCl pH 7.4) and counted using a liquid scintillation β-counter (Packard 1600 TR). The expression of Flag-β2AR, Flag-β2AR$^{SSS}$ or Flag-β2AR$^{AAA}$ was 64, 80 and 79 pmol/mg membrane protein, respectively. Expression levels of transiently transfected cells were ranging from 15 to 50 pmol/mg membrane protein.

*[$^{32}$P]Orthophosphate labeling and β2AR immunoprecipitation*

[$^{32}$P]Orthophosphate labeling, agonist incubation, receptor solubilization, immunoprecipitation and autoradiography were done as described previously (Butcher et al., 2011). Briefly, HEK 293 cells stably expressing Flag-β2-adrenoceptors were grown in six well plates. After washing and incubation with $KH_2PO_4$-free KREBS buffer (118.4 mM NaCl, 4.7 mM KCl, 4.2 mM $NaHCO_3$, 1.2 mM $MgSO_4$, 11.7 mM glucose, 10 mM HEPES, pH 7.4) containing 100 µCi/ml [$^{32}$P] orthophosphate (Perkin Elmer, Billerica, MA), cells were stimulated for 5 min with 10 µM isoprenaline. Cells were then lysed immediately (20 mM Tris, 150 mM NaCl, 3 mM EDTA, 1% IGEPAL-CA-630, pH 7.4) and immunoprecipitated using anti-Flag-M2-affinity gel. Immunoprecipitated proteins were resolved using gel electrophoresis on 8% SDS gels and visualized by autoradiography. Part of the immunoprecipitated proteins was transferred onto a PVDF membrane and subsequently immunoblotted with a polyclonal anti Flag-antibody for the detection of total receptors.

Molecular Pharmacology Fast Forward. Published on November 25, 2014 as DOI: 10.1124/mol.114.095422
This article has not been copyedited and formatted. The final version may differ from this version.



*Microscopic FRET measurements and data evaluation*

Dynamics of G-protein receptor interaction or arrestin-receptor interaction respectively were performed as previously reported (Bodmann et al., 2014; Krasel et al., 2005). In brief, 24 hrs after transfection cells were split on poly-lysine-coated 25 mm coverslips and after further 14-16 hrs analyzed by FRET microscopy using an inverted eclipse Ti Nikon microscope. Cells were maintained and continuously superfused in either FRET buffer (137 mM NaCl, 5.4 mM KCl, 2 mM $CaCl_2$, 1 mM $MgCl_2$, and 10 mM HEPES pH 7.3) or 1 µM isoprenaline in FRET buffer at room temperature using a fast switching perfusion system (Ala-VC3-8SP, ALA, Scientific Instruments). Cells were observed using a 100x oil immersion objective (Plan Apo VC 100×/1.40 NA oil, Nikon). CFP was excited with 435 nm light using an excitation filter 430/24 and a beam splitter T455LP. All filters were from Chroma. The light source was a Lambda DG4 (Sutter, Novato, CA). Some experiments were performed with an LED excitation system (pE-2, CoolLED, Andover, UK). Fluorescence emission from CFP ($F_{480}$) and YFP ($F_{535}$) were collected using an ET dual-band beam splitter CFP/YFP (59017bs Dichroic BS) emission filter $F_{480}$ 480/40, and emission filter $F_{535}$ (535/30). The illumination frequency was set to 2.5 Hz and illumination time was set to 30-40 ms to minimize photobleaching. A CCD camera (Evolve 512, Photometrics, Tucson, AZ) was used to detect the signals; FRET was calculated as $F_{YFP}/F_{CFP}$. Spillover of CFP into the YFP channel was corrected, whereas direct YFP excitation was negligible. Individual FRET recordings were averaged and are either shown as absolute alterations in FRET normalized to the baseline or normalized to the individual agonist induced response as a maximum and to the baseline as minimum, in order to display the kinetics. The dissociation and association kinetics in the presence of overexpressed GRK2 were fitted using the following monoexponential equations: dissociation: $y(t) = A \times (e^{-koff \times t}) + y_0$; association: $y(t) = A \times (1-e^{-kon \times t}) + y_0$.

Concentration-response curves for receptor-G-protein interaction were obtained by measuring amplitudes of FRET changes.

Molecular Pharmacology Fast Forward. Published on November 25, 2014 as DOI: 10.1124/mol.114.095422
This article has not been copyedited and formatted. The final version may differ from this version.



*Quantification of relative expression levels*

In experiments in which FRET amplitudes are shown, relative expression levels of fluorescently labeled proteins were determined as described before (Wolters *et al.*, 2015). In brief, both fluorophores were excited individually and background fluorescence was subtracted for each channel. The calibration factor of a reference construct YFP-β2AR-CFP (Dorsch *et al.*, 2009) was calculated as $F_{YFP}$ / $F_{CFP}$. For each individual FRET recording the factor $F_{YFP}$ / $F_{CFP}$ was calculated the same way.

*Dual color FRAP microscopy*

A protocol for arrestin-3 mobility at the plasma membrane was established based on a method that had been developed earlier in our lab (Dorsch et al., 2009). HEK 293T cells transiently expressing arrestin-3-CFP and N-terminally YFP-tagged receptors grown on coverslips were washed in BE buffer (150 mM NaCl, 2.5 mM KCl, 10 mM HEPES, 12 mM glucose, 0.5 mM $CaCl_2$ and 0.5 mM $MgCl_2$, pH 7.5) (Digby et al., 2006) followed by crosslinking N-terminally labeled receptors for 30 min at 37°C using a polyclonal GFP antibody (Rockland, Gilbertsville, PA) diluted 1:100 and supplemented with 2.5% fatty acid-free BSA. Subsequently cells were washed three times in BE buffer and maintained in the same buffer containing 10 µM isoprenaline for imaging purposes. FRAP microscopy was performed at 20°C using a Leica TCS SP5 scanning confocal microscope (Leica, Wetzlar, Germany) with a Lambda Blue 63x/1.4NA oil-immersion objective. CFP was excited at 405 nm with a diode laser and CFP emission was collected at 450-489 nm. YFP was excited at 514 nm using an argon ion laser and YFP emission was collected at 525-600 nm. The scan speed was set to 400 Hz, image format was 512x512 pixels, the zoom factor was set to 6.0 and the pinhole was set to airy 1. During bleaching in the equatorial plane of the cell membrane, laser intensity was set to 70% to achieve 60-80% loss of fluorescence in a 3x1µm rectangular area. Fluorescence recovery into the bleached membrane segment was monitored for 3-5 min at low laser intensity of 10%. Pixel intensities for CFP and YFP respectively were corrected for bleaching and CFP bleed through into the YFP channel. The lowest intensity directly after bleaching was subtracted from all other intensities after bleaching. Resulting FRAP curves were averaged, plotted as mean ± S.E. and fitted with GraphPad Prism using a two phase association: $Y = Y_0 + Span_{Fast} * (1-exp^{(-KFast*X)}) + Span_{Slow} * (1-exp^{(-KSlow*X)})$.

Molecular Pharmacology Fast Forward. Published on November 25, 2014 as DOI: 10.1124/mol.114.095422
This article has not been copyedited and formatted. The final version may differ from this version.



*μ-patterning and TIRF microscopy*

μ-contact printing was performed as reported previously (Lanzerstorfer et al., 2014). The detection system was set up on an epi-fluorescence microscope (Olympus IX81). Diode lasers (Toptica Photonics, Munich, Germany) were used for selective fluorescence excitation of CFP, YFP and Cy5 at 405 nm, 515 nm and 640 nm, respectively. The 405 nm diode laser (Toptica Photonics) was used for bleaching of YFP fluorescence (arrestin-3). Samples were illuminated in total internal reflection (TIR) configuration (CellTIRF, Olympus, Munich, Germany) using a 60 x oil immersion objective (NA = 1.49, APON 60XO TIRF, Olympus). After appropriate filtering using standard filter sets, fluorescence was imaged onto a CCD camera (Orca-R2, Hamamatsu, Japan). Samples were mounted on an x-y-stage (CMR-STG-MHIX2-motorized table; Märzhäuser, Germany) and scanning of larger areas was supported by a laser-guided automated focus-hold system (ZDC-2; Olympus). For FRAP experiments single patterns were photobleached with a laser pulse (405 nm) applied for 600 ms. Recovery images were recorded at indicated time intervals. FRAP images were analyzed using the Spotty framework (Borgmann et al., 2012). Data were normalized by the pre-bleach image and curve fitting was done using Graphpad Prism. Resulting FRAP curves were plotted based on the standard error of the mean (S. E.) and fitted using a bi-exponential equation. Kinetic FRAP parameters were directly obtained from curve fitting.

*Confocal Microscopy*

HEK293T cells grown on 6 cm dishes were transiently transfected with labeled or unlabeled Flag-β2AR, Flag-β2AR$^{SSS}$ or Flag-β2V2R, along with arrestin-3-CFP, GRK2 and mCherry-EEA1. 24 h post transfection cells were plated on 25 mm coverslips. Cells were either unstimulated or stimulated with 10 μM isoprenaline for 30 min at 37°C and then fixed with 4% paraformaldehyde. Cells expressing fluorescent proteins were examined for arrestin localization and colocalization with EEA1. Confocal images were obtained on a Leica TCS SP5 scanning confocal microscope (Leica, Wetzlar, Germany) with a Lambda Blue 63x/1.4NA oil-immersion objective. CFP was excited at 405 nm with a diode laser and CFP emission was collected at 452-543 nm. mCherry was excited at 543 nm using an HeNe laser, mCherry-emission was collected at 610-674 nm. YFP was excited at 514 nm, YFP emission was collected at 525-600 nm.

Molecular Pharmacology Fast Forward. Published on November 25, 2014 as DOI: 10.1124/mol.114.095422
This article has not been copyedited and formatted. The final version may differ from this version.



*Image analysis*

In order to measure the dependency of pixels in dual channel images we used Image J 1.47 and a colocalization plugin. Images for each channel were background subtracted and Pearson´s colocalization coefficient was calculated using the following equation: $R\,p=\frac{\sum(A_i-a)\ x\ (B_i-b)}{\sqrt{[\sum(A_i-a)^2\ x\sum(B_i-b)^2]}}$.

The channel A and channel B grey values of voxel i are noted as $A_i$ and $B_i$, respectively, and the average intensities over the full image as a and b.

*Receptor internalization and recycling*

Receptor internalization and recycling were quantified using [$^3$H]CGP12,177 (Hartmann Analytic, Braunschweig, Germany) binding. HEK293T cells transiently transfected with either Flag-β2AR or Flag-β2ARSSS were treated for 30 min at 37°C with 1 μM isoprenaline in FRET buffer containing 10 mM glucose. The cells were then chilled on ice to stop membrane trafficking and were washed for four times with ice-cold FRET buffer containing 10 mM glucose to remove the isoprenaline. Afterwards, they were allowed to recycle internalized receptor for various times at 37°C. At the end of the recycling period, cells were put on ice again and cell surface receptor was quantified by [$^3$H]CGP12,177 binding as described (Krasel *et al.*, 2005). Background binding was determined in the presence of 1 μM alprenolol.

Molecular Pharmacology Fast Forward. Published on November 25, 2014 as DOI: 10.1124/mol.114.095422
This article has not been copyedited and formatted. The final version may differ from this version.



## Results

*Agonist-induced receptor phosphorylation*

In the current study, we introduced three serine residues into the C-terminus of the β2AR 20 residues downstream from the palmitoylated Cys341 (β2AR$^{SSS}$) in analogy to the V2 vasopressin receptor which possesses a similar Ser cluster at exactly the same distance from its putative palmitoylation site (Fig. 1). It was anticipated that these residues might provide additional phosphorylation sites to those already present in this region of the receptor which would also serve to increase arrestin binding to the phosphorylated receptor (Fig.1). The phosphorylation status of this mutant receptor and that of the wild-type receptor and a control construct where alanine residues were introduced (β2AR$^{AAA}$) was determined by [$^{32}$P] metabolic labelling followed by receptor immunoprecipitation. All constructs tested showed low basal phosphorylation, which was robustly increased upon stimulation with 10 μM isoprenaline for 5 min (Fig.2A). After quantitation using densitometry, a substantial increase in receptor phosphorylation for β2AR$^{SSS}$ was observed compared to β2AR (Fig.2B), suggesting that the additional serine residues are phosphorylated in an agonist-dependent manner, a conclusion supported by the fact that phosphorylation of the β2AR$^{AAA}$ construct appeared similar to β2AR levels.

*$G_s$-protein coupling*

To investigate whether the introduction of the three serine residues would alter the coupling of the β2AR to $G_s$-protein, a FRET-based assay was used to evaluate the interaction between the receptor and the Gβγ subunit of the heterotrimeric $G_s$-protein upon receptor activation (Hein *et al.*, 2005). In these experiments HEK293T cells transiently transfected with various β2ARs and the three $G_s$ subunits were superfused with isoprenaline at concentrations ranging from 100 pM to 10 μM (Fig. 3A). In this assay, levels of receptor and $G_s$ are increased and most probably in excess of endogenous arrestin, therefore little receptor desensitization is expected. The wild-type β2AR showed $G_s$-protein activation with an $EC_{50}$ value of 9.8 nM (Fig. 3B). A mutant receptor in which 12 phosphorylation sites had been mutated to alanine or glycine to generate a receptor that was significantly reduced in agonist-mediated phosphorylation (β2AR$^{pd}$; see Fig. 1 for sequence) (Bouvier *et al.*, 1988) showed activation of $G_s$-protein that was not significantly different from the wild-type

Molecular Pharmacology Fast Forward. Published on November 25, 2014 as DOI: 10.1124/mol.114.095422
This article has not been copyedited and formatted. The final version may differ from this version.



receptor ($EC_{50}$ = 7.7 nM) (Fig. 3B). $G_s$-protein activation via the $\beta2AR^{SSS}$ mutant receptor occurred at slightly higher agonist concentrations but was not significantly different from the wild-type receptor ($EC_{50}$ = 25.8 nM) (Fig. 3B). These data indicate that G-protein coupling is not adversely affected in the $\beta2AR^{SSS}$ mutant.

*Receptor phosphorylation and interaction with arrestin*

β2-adrenoceptors recruit arrestins in a phosphorylation-dependent manner. The removal of phospho-acceptor sites within the proximal C-terminal tail of the β2AR leads to a marked attenuation of arrestin-3 binding, whereas the more distal phosphorylation sites in the C-terminal tail do not influence the affinity of arrestin-3 for the receptor (Krasel et al., 2008; Seibold et al., 1998). In order to monitor the association and dissociation kinetics of arrestin-receptor interaction, we used a FRET-based assay employing arrestin-3 and β2AR tagged with YFP and CFP, respectively (Krasel *et al.*, 2005). The association constant for $\beta2AR^{AAA}$ was slowed significantly compared to β2AR and the $\beta2AR^{SSS}$ (Fig. 4A, table 1). More importantly, the off-rate of the β2AR was significantly reduced in the $\beta2AR^{SSS}$ mutant (Fig. 4A, B, table 1). Furthermore, whereas arrestin-3 almost completely dissociated from the wild-type receptor during the time course of the experiment, dissociation of arrestin-3 from the $\beta2AR^{SSS}$ was significantly reduced (Fig. 4A, table 1). In contrast, arrestin-3 interaction with β2V2R was nearly irreversible as only a small portion of the previously bound arrestin-3 actually dissociated on the timescale of the experiment (Fig 4A, table 1). However, the fraction of arrestin-3 which dissociated from the β2V2R did so with faster kinetics compared to $\beta2AR^{SSS}$ (Fig. 4A, B, table 1). Importantly, the off-rate of the $\beta2AR^{AAA}$ was similar to that of the wild-type β2AR (Fig. 4A and B, table 1). Hence, it appeared that the introduction of phosphorylation sites into the β2AR increased its affinity for arrestin-3 as shown by a decrease in the rate and extent of dissociation.

The data above were measured in the presence of overexpressed GRK2. We also tested whether the observed differences arrestin-3 dissociation kinetics were still present with endogenous GRK levels. In cells not transfected with GRK2 the rate of arrestin-3 dissociation from the wild-type receptor was not significantly different from that of cells over-expressing GRK2 (compare Fig. 4B and D). Importantly, the $\beta2AR^{SSS}$ mutant receptor still demonstrated a significantly slower rate of dissociation compared to the wild-type β2AR in the cells expressing endogenous levels of GRK

Molecular Pharmacology Fast Forward. Published on November 25, 2014 as DOI: 10.1124/mol.114.095422
This article has not been copyedited and formatted. The final version may differ from this version.



(Fig. 4C, D table 1). We relate the ability of the β2AR$^{SSS}$ to bind arrestin with enhanced affinity to the insertion of the triple S cluster and its phosphorylation. To ascribe the enhanced phosphorylation shown in Fig. 2A to phosphorylation of one or more of the introduced sites we assessed the phosphorylation of a β2AR that contains solely the 3S cluster (β2AR 3S); all other potential GRK phosphorylation sites were mutated to glycine or alanine (see Fig.1 for sequences). To exclude the possibility of PKA phosphorylation we stimulated the cells in the presence of the PKA inhibitor KT5720 and compared agonist-dependent receptor phosphorylation between β2AR 2S, β2AR 3S, β2AR 5S and β2AR pd. The β2AR 3S showed a substantial increase in ligand-dependent phosphorylation that was similar to the increase in the phosphorylation of β2AR 2S (Fig. 5A, B), suggesting that at least one or two of the serines within the 3S cluster can become phosphorylated in an agonist-dependent manner. The largest increase in phosphorylation was observed upon stimulation of a receptor that contains Ser 355, 356 and the SSS cluster in combination which further confirmed the assumption that the triple S cluster serves as a substrate for GRKs. To examine the phosphorylation dependence of arrestin recruitment we determined the raise in the FRET signal with β2ARs with increasing numbers of serines, as described above (Fig 5C). No direct interaction between arrestin and the β2AR$^{pd}$ could be detected in FRET, confirming previous results (Krasel et al., 2005). However, introducing either S$^{355}$ and S$^{356}$ or replacing residues 361-363 (GEQ) with SSS both led to a marked increase in FRET which was further enhanced when both serine motifs in combination were present (Fig. 5C). To rule out the possibility that the increase in the amplitude of the FRET signal resulted from unequal relative expression levels of β2ARs and arrestin-3, we determined the relative expression levels as described in the methods section and as shown in Fig. 5D. We found no significant difference in the stoichiometry of the fluorescently labeled proteins, indicating that the number of phosphorylation sites determines the extent of the arrestin interaction with receptors.

Molecular Pharmacology Fast Forward. Published on November 25, 2014 as DOI: 10.1124/mol.114.095422
This article has not been copyedited and formatted. The final version may differ from this version.



*Influence of a distal SSS cluster on arrestin affinity*

In order to analyze the relevance of the localization of the 3S cluster we replaced three residues 397-399 (NID) within the β2AR with serines (β2AR SSS distal, Fig. 1) and determined the arrestin interaction using FRET. The arrestin dissociation kinetics were very similar for β2AR and β2AR SSS distal as both traces were superimposable after ligand washout (Supplemental Figure 1 A and B). The comparison of these data to the dissociation kinetics from the β2AR with the SSS cluster in the proximal part of the C-terminal tail (Supplemental Figure 1 B) revealed that arrestin shows enhanced affinity towards a receptor with the proximal SSS cluster but not towards a receptor that offers the same cluster with a total of four consecutive serines in the distal part of the tail.

*Arrestin-receptor interaction in the continuous presence of agonist*

During agonist washout, the receptor undergoes a conformational change from an activated into a non-activated state. Arrestin senses this conformational change and dissociates from the receptor (Krasel *et al.*, 2005). To investigate whether arrestin affinity for the active state of the receptor is changed by the addition of phospho-acceptor sites to the C-terminal tail of the receptor, we established an assay based on dual color fluorescence recovery after photobleaching (FRAP) to monitor the kinetics of association and dissociation of arrestin-3 to agonist-bound β2AR, β2AR$^{SSS}$ or β2V2R. All receptor constructs used in this assay were N-terminally tagged with YFP and were observed in single live cells. Receptors were immobilized at the membrane by crosslinking them with a polyclonal YFP-antibody (Dorsch et al., 2009). Subsequently, receptors were stimulated with 10 μM isoprenaline causing arrestin-3-CFP translocation to receptors. A small region of interest (3x1μm) at the plasma membrane was photobleached using high laser intensity and the re-distribution of both immobilized receptors and arrestin-3 was monitored simultaneously using low laser intensity (Fig. 6A, B). Antibody crosslinking treatment reduced the mobility of the receptors by reducing the lateral diffusion of receptor-arrestin complexes such that receptor recovery was ~20% for all three receptor constructs (Fig. 6D) compared to more than 50% for non-crosslinked receptor (Fig. 6F). The recovery of fluorescent arrestin-3 into the bleached area is therefore a result of arrestin-3 dissociation from and re-association to immobile receptors. We found that this recovery could be quantified by a two-phase association. Figure 6C shows the mean recovery ± S.E. of

Molecular Pharmacology Fast Forward. Published on November 25, 2014 as DOI: 10.1124/mol.114.095422
This article has not been copyedited and formatted. The final version may differ from this version.



arrestin-3 with β2AR, β2AR$^{SSS}$ or β2V2R and table 1 summarizes the time constants $k_{fast}$ , $k_{slow}$ and corresponding $t_{0.5}$ values as well as the extent of the arrestin-3 recovery. The three β2AR constructs all showed differences in the kinetics of arrestin-3 recovery. The slow recovery rate of arrestin-3 for the β2AR$^{SSS}$ construct was reduced about 1.5fold compared to the β2AR (Fig. 6D) whereas the extent of recovery was unchanged. In contrast, the recovery rate for the β2V2R was slowed down more than 3fold compared to the β2AR, and the extent of recovery was reduced 2.5fold compared to the β2AR (Fig. 6B, D, table 1).

In addition, we determined the arrestin-3 recovery after photobleaching to Flag-β2AR or Flag-β2AR$^{SSS}$ on μ-patterned surfaces using TIRF microscopy in HeLa cells to study the mobility of arrestin-3 clusters at the cell surface. Figure 7A shows an example of μ-patterned Flag-β2AR-CFP. Unstimulated receptors (upper panel) showed low levels of arrestin-3 clustering of arrestin-3 whereas arrestin-3 clustering was robustly increased upon stimulation with 10μM isoprenaline (Fig. 7A lower panel). Increased clustering and colocalization of arrestin-3 in receptor-enriched μ-patterns was quantified by contrast evaluation (Fig. 7B). The arrestin-3-YFP recovery after photobleaching was slowed 3 fold for the β2AR$^{SSS}$ compared to β2AR (Fig. 7C, upper panel vs. lower panel and D, E).

*Arrestin-3 trafficking*

We next set out to investigate how the introduction of additional phospho-acceptor sites within the β2AR C-terminus might change the trafficking pattern of arrestin-3. Isoprenaline stimulation of YFP-tagged β2AR, β2AR$^{SSS}$ or β2V2R increased receptor internalization in all cases (Fig. 8A, middle panel). After 30 min of β2AR stimulation, arrestin-3 was found either redistributed into the cytosol or at or near to the plasma membrane (Fig. 8A, upper panel, left), whereas upon β2AR$^{SSS}$ or β2V2R activation arrestin was found on intracellular vesicles (Fig. 8A middle and lower left panel). The intracellular cotrafficking of arrestin with receptors was quantified by using Pearson´s correlation coefficient as described in the methods section. Quantification of the cotrafficking showed that the endocytic colocalization of arrestin with β2AR$^{SSS}$ and the β2V2R as a control was markedly enhanced compared to β2AR (Fig 8B).

To further characterize the arrestin-3 trafficking, β2AR, β2AR$^{SSS}$ or β2V2R were stimulated with isoprenaline and arrestin-3 was analyzed for colocalization with early endosome antigen 1 (EEA1) which is a specific marker for early endosomes

Molecular Pharmacology Fast Forward. Published on November 25, 2014 as DOI: 10.1124/mol.114.095422
This article has not been copyedited and formatted. The final version may differ from this version.



(Stenmark et al., 1996). Stimulation of β2AR with 10 μM isoprenaline resulted in translocation of arrestin-3-CFP to the plasma membrane which remained unchanged over 30 min period of observation (Fig. 9A, upper panel). In contrast, stimulation of the $\beta2AR^{SSS}$ (Fig. 9A, middle panel) and β2V2R (Fig. 9A, lower panel) caused internalization of arrestin-3-CFP into EEA1-positive compartments. Colocalization was quantified using Pearson´s correlation coefficient and identified significant differences between arrestin-3 trafficking with $\beta2AR^{SSS}$ and β2V2R compared to β2AR (Fig. 9B).

To clarify whether the presence of the triple S cluster in combination with Ser 355/ 356 (β2AR 5S) is able to induce endosomal cotrafficking with arrestin, we performed additional trafficking experiments with this mutant (Supplemental Figure 2). After 30 min of agonist incubation no overlap of arrestin with EEA1 could be observed (Supplemental Figure 2, lower panel). These data suggest that the SSS cluster is required in addition to the full pattern of serines and threonines in the proximal part of the tail, but not sufficient for the cointernalization of arrestin and β2AR.

*Internalization and recycling of β2AR and $\beta2AR^{SSS}$*

We next investigated whether the enhanced arrestin affinity towards the SSS cluster in the proximal part of the β2AR was associated with altered internalization or recycling of receptors. Ligand-dependent internalization of the β2AR is an arrestin-dependent process; therefore we hypothesized that a receptor that possesses the ability to bind arrestin stronger might show alterations in its internalization properties. Indeed, the $\beta2AR^{SSS}$ internalized significantly more efficiently (30 ± 4.5%) than the wild-type receptor (13.5 ± 4.6%; Fig. 10 A) after 30 min of treatment with 1 μM isoprenaline. Similar results for β2AR internalization in the absence of overexpressed arrestin have been published before (Kim and Benovic, 2002). After 30 min of stimulation the agonist was removed by repetitive washing steps and receptors were allowed to recycle for the indicated time points (Fig. 10). Both β2AR and $\beta2AR^{SSS}$ recycled rapidly by ~60% within 30 min. Very similar results for the recycling of wild-type β2AR without subsequent antagonist treatment have been observed before (Gage *et al.*, 2001).

Molecular Pharmacology Fast Forward. Published on November 25, 2014 as DOI: 10.1124/mol.114.095422
This article has not been copyedited and formatted. The final version may differ from this version.



## Discussion

For many GPCRs, agonist-dependent receptor phosphorylation results in arrestin recruitment and subsequent internalization. Arrestin can either dissociate from the receptor very shortly after internalization, giving the appearance of plasma membrane staining, or co-internalize with the receptor into endosomes. Based on work with receptor chimeras it has been suggested that this trafficking behaviour depends on the number of Ser and/or Thr residues in the C-terminus of the receptor (Oakley et al., 2000; Pal et al., 2013). However, swapping the entire C-terminus of the receptor will not only affect arrestin trafficking but other receptor properties as well, such as recycling (Cao *et al.*, 1999). Therefore we examined whether the insertion of just three additional serine phospho-acceptor sites 20 amino acids away from the plasma membrane ($\beta2AR^{SSS}$) could induce any changes regarding receptor phosphorylation, arrestin affinity and trafficking. Firstly, we investigated whether the addition of three serines within the $\beta2AR^{SSS}$ leads to an increase in total receptor phosphorylation. Secondly, we monitored G-protein coupling, arrestin-3 recruitment and dissociation in real time. In addition we analyzed arrestin-3 trafficking behavior as well as receptor internalization and recycling in response to this mutation. We demonstrate that the addition of phospho-acceptor sites to the proximal C-terminus of the β2AR led to increased agonist-induced phosphorylation which was accompanied by enhanced stability of arrestin-3-receptor complexes and arrestin-3 localization on endosomes.

Using FRET we measured the interaction of heterotrimeric G-proteins with β2AR in a dose-dependent manner and found no significant differences for the $EC_{50}$ values of isoprenaline-induced G-protein interaction with β2AR, $\beta2AR^{SSS}$ or $\beta2AR^{pd}$ (Fig.3). These results suggest that the initial phase of G-protein coupling occurs independently from receptor phosphorylation and compare favorably with those reported in the literature (Benovic *et al.*, 1987; Lohse *et al.*, 1992).

The real-time observation of arrestin-3 recruitment using FRET revealed that upon stimulation with 1 µM isoprenaline, arrestin-3 was recruited to β2AR, $\beta2AR^{SSS,}$ $\beta2AR^{AAA}$ or β2V2R. The differing recruitment kinetics probably reflect subtle differences in the ability of the various receptors to be phosphorylated by GRK2. During agonist washout, the receptor undergoes a conformational change from an activated into a non-activated state. Arrestin is able to sense this conformational

Molecular Pharmacology Fast Forward. Published on November 25, 2014 as DOI: 10.1124/mol.114.095422
This article has not been copyedited and formatted. The final version may differ from this version.



change and dissociates from the receptor (Krasel et al., 2005). The arrestin-3 dissociation kinetics from a typical class A receptor, such as the β2AR, proceeded quickly and almost completely, whereas the dissociation rate from the class B receptor β2V2R (Oakley et al., 1999) was delayed and considerably smaller (Fig. 4A). Interestingly, the interaction of arrestin-3 with the β2AR$^{SSS}$ construct was significantly prolonged by a factor of 2.5 and the fraction of arrestin which dissociated after ligand washout was reduced by half. Hence, the kinetic data presented here provide some evidence that different phosphorylation states of receptors can be detected by arrestin-3 and these are reflected in the arrestin dissociation rate that we have measured here in real time. As the affinity to the receptor remained unchanged by the addition of a SSS cluster to the distal part of the tail (Supplemental Figure 1), this confirms that arrestin senses phosphorylation specifically in the proximal part of the C-terminal tail.

We extended our study further by asking whether the addition of phospho-acceptor sites to the receptor C-tail can also alter the arrestin-3 affinity for the activated receptor. Dual color fluorescence recovery after photobleaching (FRAP) was used here to monitor the kinetics of association and dissociation of arrestin-3 to immobilized agonist-bound β2AR, β2V2R, and β2AR$^{SSS}$ in single living cells. The arrestin-3 recovery after photobleaching reflects two processes, the remaining lateral diffusion of receptor-arrestin-3 complexes and the release of arrestin-3 from immobilized receptors followed by subsequent rebinding of free arrestin-3. The β2AR$^{SSS}$ showed approximately 2.2 fold slower fluorescence recovery than the β2AR in HEK293 cells using confocal microscopy and approximately 4 fold slower fluorescence recovery in HeLa cells using TIRF microscopy. These differences in the kinetics and the extent of arrestin-3-recovery in the equatorial plane of the membrane or at the cell surface reflect its stability in complex with the various receptors investigated in this study. Thus, the temporal stability of arrestin-3-receptor complexes in the presence or in the absence of agonist is determined by the extent and possibly the pattern of receptor phosphorylation that is present in the proximal part of the receptor´s C-terminal tail. The slow kinetics of arrestin-3 recovery for the β2AR$^{SSS}$ were more pronounced using TIRF microscopy. We assume that this could be related to the larger area that was photobleached on the cell surface (7 μm$^2$, circle) compared to area that was photobleached within the equatorial plane of the membrane (3x1μm, rectangle).

Molecular Pharmacology Fast Forward. Published on November 25, 2014 as DOI: 10.1124/mol.114.095422
This article has not been copyedited and formatted. The final version may differ from this version.



We and others have shown that the number of phosphorylated residues on receptors determines the nature of the complex formed with arrestins (Krasel et al., 2008; Vishnivetskiy et al., 2007). The kinetic modeling of arrestin-3 with β2AR or β2AR$^{SSS}$ via FRET or FRAP suggests that very likely the phosphorylation of the additional serine cluster leads to a 2- to 4 fold enhancement in the stability of the complex between arrestin-3 and β2AR$^{SSS}$ compared to the nature of the complex formed with β2AR that appears to be rather transient. Different phosphorylation patterns elicited by different GRKs or arising from stimulation with distinct ligands have been proposed to impart differential arrestin conformations responsible for the fine-tuning of subsequent signaling events (Nobles et al., 2011). We show here that the removal of all phosphosites in the proximal C-terminus almost abolishes arrestin binding whereas arrestin interaction was restored to some extent by the addition of two or three phosphosites; it did not seem to play a role in which exact position these serines were present, as the extent of arrestin interaction was very similar for β2AR 2S and β2AR 3S. The combination of the 3S cluster and Ser 355/356 (β2AR 5S) improved arrestin binding markedly, however the arrestin affinity was less pronounced with β2AR 5S compared to β2AR$^{SSS}$, suggesting that the full range of serines in addition to the SSS cluster is required to switch the characteristics of this receptor. The β2AR$^{SSS}$ mutant appeared to show characteristics of a class B receptor, a class of GPCRs which have previously been proposed to interact strongly with arrestin (Oakley et al., 2000). Previous studies have shown that the β2AR could be converted from a class A to a class B receptor by substituting the C-terminal tail of the receptor with the C-tail of the V2-vasopressin receptor (Oakley et al., 1999). Arrestin-3 dissociates from this chimeric receptor more quickly than from the β2AR$^{SSS}$ mutant, and both mutants show a reduced extent of arrestin dissociation on the timescale of the experiment compared to wild-type (Fig. 4A and B), supporting the notion that by increasing the number of phosphorylation sites on the β2AR the receptor is converted from a class A to a class B receptor. Although the β2AR$^{SSS}$ showed class B behavior in terms of arrestin binding it did not in terms of recycling. However, it has been shown previously (Cao *et al.*, 1999) that rapid recycling of the β2AR was mediated by binding of EPB50 to phosphorylated Ser 411 and the PDZ domain in the distal part of the C-terminal tail, as the distal part was not changed in the β2AR$^{SSS}$ it is not unexpected that this receptor displays the same recycling properties as the wild-type receptor.

Molecular Pharmacology Fast Forward. Published on November 25, 2014 as DOI: 10.1124/mol.114.095422
This article has not been copyedited and formatted. The final version may differ from this version.



Our data suggest that arrestin can form structurally and functionally differential complexes dependent on the number of phosphorylation sites in the proximal part of the C-terminal tail. In summary, the experiments in this report demonstrate that a 2-4 fold increase in the stability of the arrestin-3-β2AR$^{SSS}$ interaction compared to the stability of β2AR-arrestin-3 complex has a profound impact on the internalization behavior of β2AR$^{SSS}$ and its trafficking properties with arrestin-3.

Molecular Pharmacology Fast Forward. Published on November 25, 2014 as DOI: 10.1124/mol.114.095422
This article has not been copyedited and formatted. The final version may differ from this version.



**Acknowledgements**

We thank Nicholas Holliday and Simon Davies (University of Nottingham) for providing the cDNA for EEA1-GFP. We are grateful to Prof. Gerhard Schratt and Dr. Christian Wrocklage for access to the isotope lab and to the Leica SP5 microscope.

**Author contributions**

Participated in research design: Zindel, Butcher, Al-Sabah, Weghuber, Tobin, Bünemann, Krasel

Conducted experiments: Zindel, Butcher, Lanzerstorfer, Krasel

Contributed new reagents or analytic tools: Zindel, Al-Sabah, Krasel

Performed data analysis: Zindel, Lanzerstorfer, Bünemann, Krasel

Wrote or contributed to the writing of the manuscript: Zindel, Butcher, Tobin, Krasel

Molecular Pharmacology Fast Forward. Published on November 25, 2014 as DOI: 10.1124/mol.114.095422
This article has not been copyedited and formatted. The final version may differ from this version.



## References

Benovic JL, Kühn H, Weyand I, Codina J, Caron MG and Lefkowitz RJ (1987) Functional desensitization of the isolated beta-adrenergic receptor by the beta-adrenergic receptor kinase: potential role of an analog of the retinal protein arrestin (48-kDa protein). *Proc Natl Acad Sci USA* **84**: 8879-8882.

Bodmann EL, Rinne A, Brandt D, Lutz S, Wieland T, Grosse R and Bünemann M (2014) Dynamics of Gαq-protein-p63RhoGEF interaction and its regulation by RGS2. *Biochem J* **458**: 131-140.

Borgmann DM, Weghuber J, Schaller S, Jacak J and Winkler SM (2012) Identification of patterns in microscopy images of biological samples using evolution strategies., in *Proceedings of the 24th European Modeling and Simulation Symposium* pp 271-276, Vienna.

Bouvier M, Hausdorff WP, De Blasi A, O'Dowd BF, Kobilka BK, Caron MG and Lefkowitz RJ (1988) Removal of phosphorylation sites from the $\beta_2$-adrenergic receptor delays onset of agonist-promoted desensitization. *Nature* **333**: 370-373.

Butcher AJ, Prihandoko R, Kong KC, McWilliams P, Edwards JM, Bottrill A, Mistry S and Tobin AB (2011) Differential G-protein-coupled receptor phosphorylation provides evidence for a signaling bar code. *J Biol Chem* **286**: 11506-11518.

Cao TT, Deacon HW, Reczek D, Bretscher A and von Zastrow M (1999) A kinase-regulated PDZ-domain interaction controls endocytic sorting of the $\beta_2$-adrenergic receptor. *Nature* **401**: 286-290.

Digby GJ, Lober RM, Sethi PR and Lambert NA (2006) Some G protein heterotrimers physically dissociate in living cells. *Proc Natl Acad Sci USA* **103**: 17789-17794.

Doan T, Mendez A, Detwiler PB, Chen J and Rieke F (2006) Multiple phosphorylation sites confer reproducibility of the rod's single-photon responses. *Science* **313**: 530-533.

Dorsch S, Klotz K-N, Engelhardt S, Lohse MJ and Bünemann M (2009) Analysis of receptor oligomerization by FRAP microscopy. *Nat Methods* **6**: 225-230.

Frank M, Thümer L, Lohse MJ and Bünemann M (2005) G Protein activation without subunit dissociation depends on a $G\alpha_i$-specific region. *J Biol Chem* **280**: 24584-24590.

Gage RM, Kim K-A, Cao TT and von Zastrow M (2001) A transplantable sorting signal that is sufficient to mediate rapid recycling of G protein-coupled receptors. *J Biol Chem* **276**: 44712-44720.

Hall RA, Premont RT, Chow CW, Blitzer JT, Pitcher JA, Claing A, Stoffel RH, Barak LS, Shenolikar S, Weinman EJ, Grinstein S and Lefkowitz RJ (1998) The $\beta_2$-adrenergic receptor interacts with the $Na^+/H^+$-exchanger regulatory factor to control $Na^+/H^+$ exchange. *Nature* **392**: 626-630.

Hein P, Rochais F, Hoffmann C, Dorsch S, Nikolaev VO, Engelhardt S, Berlot CH, Lohse MJ and Bünemann M (2006) $G_s$ activation is time-limiting in initiating receptor-mediated signaling. *J Biol Chem* **281**: 33345-33351.

Karoor V, Wang L, Wang H-y and Malbon CC (1998) Insulin stimulates sequestration of β-adrenergic receptors and enhanced association of β-adrenergic receptors with Grb2 via tyrosine 350. *J Biol Chem* **273**: 33035-33041.

Krasel C, Bünemann M, Lorenz K and Lohse MJ (2005) β-Arrestin binding to the $\beta_2$-adrenergic receptor requires both receptor phosphorylation and receptor activation. *J Biol Chem* **280**: 9528-9535.

Krasel C, Dammeier S, Winstel R, Brockmann J, Mischak H and Lohse MJ (2001) Phosphorylation of GRK2 by protein kinase C abolishes its inhibition by calmodulin. *J Biol Chem* **276**: 1911-1915.

Krasel C, Zabel U, Lorenz K, Reiner S, Al-Sabah S and Lohse MJ (2008) Dual role of the $\beta_2$-adrenergic receptor C terminus for the binding of β-arrestin and receptor internalization. *J Biol Chem* **283**: 31840-31848.

Lanzerstorfer P, Borgmann D, Schutz G, Winkler SM, Hoglinger O and Weghuber J (2014) Quantification and kinetic analysis of Grb2-EGFR interaction on micro-patterned surfaces for the characterization of EGFR-modulating substances. *PLoS One* **9**: e92151.

Lohse MJ, Andexinger S, Pitcher J, Trukawinski S, Codina J, Faure JP, Caron MG and Lefkowitz RJ (1992) Receptor-specific desensitization with purified proteins. Kinase dependence and receptor specificity of β-arrestin and arrestin in the $\beta_2$-adrenergic receptor and rhodopsin systems. *J Biol Chem* **267**: 8558-8564.

Lutz S, Freichel-Blomquist A, Yang Y, Rümenapp U, Jakobs KH, Schmidt M and Wieland T (2005) The guanine nucleotide exchange factor p63RhoGEF, a specific link between $G_{q/11}$-coupled receptor signaling and RhoA. *J Biol Chem* **280**: 11134-11139.

Nobles KN, Xiao K, Ahn S, Shukla AK, Lam CM, Rajagopal S, Strachan RT, Huang T-Y, Bressler EA, Hara MR, Shenoy SK, Gygi SP and Lefkowitz RJ (2011) Distinct phosphorylation sites on the $\beta_2$-adrenergic receptor establish a barcode that encodes differential functions of β-arrestin. *Sci Signal* **4**: ra51.

Oakley RH, Laporte SA, Holt JA, Barak LS and Caron MG (1999) Association of β-arrestin with G protein-coupled receptors during clathrin-mediated endocytosis dictates the profile of receptor resensitization. *J Biol Chem* **274**: 32248-32257.

Oakley RH, Laporte SA, Holt JA, Barak LS and Caron MG (2001) Molecular determinants underlying the formation of stable intracellular G protein-coupled receptor-β-arrestin complexes after receptor endocytosis. *J Biol Chem* **276**: 19452-19460.

Oakley RH, Laporte SA, Holt JA, Caron MG and Barak LS (2000) Differential affinities of visual arrestin, βarrestin1, and βarrestin2 for G protein-coupled receptors delineate two major classes of receptors. *J Biol Chem* **275**: 17201-17210.

Pal K, Mathur M, Kumar P and DeFea K (2013) Divergent β-arrestin-dependent signaling events are dependent upon sequences within G-protein-coupled receptor C termini. *J Biol Chem* **288**: 3265-3274.

Pitcher JA, Freedman NJ and Lefkowitz RJ (1998) G protein-coupled receptor kinases. *Annu Rev Biochem* **67**: 653-692.

Ren X-R, Reiter E, Ahn S, Kim J, Chen W and Lefkowitz RJ (2005) Different G protein-coupled receptor kinases govern G protein and β-arrestin-mediated signaling of V2 vasopressin receptor. *Proc Natl Acad Sci USA* **102**: 1448-1453.

Seibold A, January BG, Friedman J, Hipkin RW and Clark RB (1998) Desensitization of $\beta_2$-adrenergic receptors with mutations of the proposed G protein-coupled receptor kinase phosphorylation sites. *J Biol Chem* **273**: 7637-7642.

Seibold A, Williams B, Huang Z-F, Friedman J, Moore RH, Knoll BJ and Clark RB (2000) Localization of the sites mediating desensitization of the $\beta_2$-adrenergic receptor by the GRK pathway. *Mol Pharmacol* **58**: 1162-1173.

Stenmark H, Aasland R, Toh BH and D'Arrigo A (1996) Endosomal localization of the autoantigen EEA1 is mediated by a zinc-binding FYVE finger. *J Biol Chem* **271**: 24048-24054.

Tobin AB, Butcher AJ and Kong KC (2008) Location, location, location...site-specific GPCR phosphorylation offers a mechanism for cell-type-specific signalling. *Trends Pharmacol Sci* **29**: 413-420.

Tohgo A, Choy EW, Gesty-Palmer D, Pierce KL, Laporte S, Oakley RH, Caron MG, Lefkowitz RJ and Luttrell LM (2003) The stability of the G protein-coupled receptor-β-arrestin interaction determines the mechanism and functional consequence of ERK activation. *J Biol Chem* **278**: 6258-6267.

Vaughan DJ, Millman EE, Godines V, Friedman J, Tran TM, Dai W, Knoll BJ, Clark RB and Moore RH (2006) Role of the G protein-coupled receptor kinase site serine cluster in $\beta_2$-adrenergic receptor internalization, desensitization, and β-arrestin translocation. *J Biol Chem* **281**: 7684-7692.

Vishnivetskiy SA, Raman D, Wei J, Kennedy MJ, Hurley JB and Gurevich VV (2007) Regulation of arrestin binding by rhodopsin phosphorylation level. *J Biol Chem* **282**: 32075-32083.

Wolters V, Krasel C, Brockmann J and Bünemann M (2015) Influence of $G\alpha_q$ on the dynamics of M3-acetylcholine receptor-G protein-coupled receptor kinase 2 interaction. *Mol Pharmacol* **87**: 9-17.

Zidar DA, Violin JD, Whalen EJ and Lefkowitz RJ (2009) Selective engagement of G protein coupled receptor kinases (GRKs) encodes distinct functions of biased ligands. *Proc Natl Acad Sci USA* **106**: 9649-9654.

Molecular Pharmacology Fast Forward. Published on November 25, 2014 as DOI: 10.1124/mol.114.095422
This article has not been copyedited and formatted. The final version may differ from this version.



## Footnotes

This work was supported by the Deutsche Forschungsgemeinschaft as part of the project A13 of the SFB593 ‘Mechanisms of cellular compartimentalisation and the relevance for disease’. Part of this work was supported by a BBSRC new investigator grant to CK [Grant BB/D012902/1]. DZ was the recipient of a DAAD PROMOS Travel Grant. AJB and ABT are funded by a MRC programme leader grant through the MRC Toxicology Unit.

Molecular Pharmacology Fast Forward. Published on November 25, 2014 as DOI: 10.1124/mol.114.095422
This article has not been copyedited and formatted. The final version may differ from this version.



## Figure legends

*Figure 1. Sequence alignment of the human* β2AR *variants used in this study.*
Shown are all residues of the β2AR starting at phenylalanine 336, which is located at the beginning of the intracellular C-terminal tail. Amino acids used for replacement are underlined and highlighted in the corresponding mutant sequences in bold. In the β2V2R the entire C-terminus of the β2AR was replaced by the C-terminus of the vasopressin type 2 receptor.

*Figure 2. $^{32}P$ incorporation after isoprenaline treatment*
(A) HEK 293 cells stably expressing either Flag-β2AR, Flag-$\beta2AR^{SSS}$, or Flag-$\beta2AR^{AAA}$ were immunoprecipitated and phosphorylated proteins identified by autoradiography (upper panel); equal receptor expression was confirmed by Western blotting (lower panel). (B) Quantification of agonist-induced phosphorylation as presented in A. Results are mean ± S.E. of 3-5 independent experiments $^{**}p < 0.01$, ANOVA followed by Dunnett´s multiple comparison test.

*Figure 3. Analysis of receptor G-protein interaction by FRET*
(A) HEK293T cells transiently expressing β2AR-YFP, $\beta2AR^{SSS}$-YFP or $\beta2AR^{pd}$-YFP and $G\alpha_s$, $G\beta_1$-Cer and $G\gamma_2$ were stimulated with different concentrations of isoprenaline. Representative FRET traces showing the β2AR-YFP interaction with $G\beta_1$-Cer upon stimulation with different concentrations of isoprenaline. (B) Concentration-response curves of receptor/G-protein interactions for β2AR, $\beta2AR^{SSS}$, or $\beta2AR^{pd}$ (n=7-9) were obtained by evaluating the amplitudes of FRET changes. FRET responses following stimulation with 1 μM isoprenaline were set to 100%. Individual curves to obtain $EC_{50}$ values were fitted using a sigmoidal dose response equation with constant hill slope=1, statistics of obtained EC 50 values was done with ANOVA followed by Bonferroni´s multiple comparison test $p>0.05$.

Molecular Pharmacology Fast Forward. Published on November 25, 2014 as DOI: 10.1124/mol.114.095422
This article has not been copyedited and formatted. The final version may differ from this version.



*Figure 4. Differential arrestin-3 affinities to β2-adrenoceptors with varying receptor-C-terminal tails upon agonist washout measured in real time by FRET.*

(A) Summarized data for arrestin-3-interaction with β2AR, β2AR$^{SSS}$, β2AR$^{AAA}$ or β2V2R. HEK293T cells were transiently transfected with arrestin-3-CFP, GRK2 and either C-terminally YFP-tagged Flag-β2AR, Flag-β2V2R, Flag-β2AR$^{SSS}$ or Flag-β2AR$^{AAA}$. Dynamics of arrestin-3 interaction with receptors were determined by measuring FRET. Cells were perfused with FRET buffer for 30 s, followed by 1 μM isoprenisoprenaline for 180 s, followed by FRET buffer for 180 s. On-rates were determined by curve-fitting to a single exponential equation. Statistics were performed by Kruskal Wallis test followed by Dunn´s multiple comparison test. ***p<0.001 (β2AR$^{AAA}$ vs β2AR$^{SSS}$) **p<0.01 (β2AR vs β2AR$^{AAA}$). (B) Calculated $k_{off}$ ± S.E. of arr-3-receptor dissociation upon agonist washout and corresponding $t_{0.5}$ values (within the bars). Off-rates were fitted to a single exponential equation and statistics were performed by Kruskal Wallis test followed by Dunn´s multiple comparison test. ***p<0.001, **p<0.01, *p<0.05. (C) HEK 293T cells transiently transfected with β2AR-YFP or β2AR$^{SSS}$-YFP and arr-3-CFP were measured and the data summarized as described in (A). (D) $k_{off}$ ±S.E. and corresponding $t_{0.5}$ values (within the bars), Student´s t-test, **p<0.01.

*Figure 5. Number of phosphorylation sites within the β2AR determines the extent of ligand dependent interaction of arrestin-3.*

(A) HEK 293T cells transiently expressing β2 receptors with the indicated number of possible phosphorylation sites were preincubated for 30 min with 1μM of the PKA inhibitor KT 5720. Isoprenaline-challenged receptors were immunoprecipitated and phosphorylated proteins were visualized by autoradiography (upper panel); receptor expression was shown by Western blotting (lower panel). (B) Quantification of ligand-induced phosphorylation as presented in A. Results are mean ± S.E. of three independent experiments, *** p < 0.001; ** p < 0.01; * p< 0.05. ANOVA followed by Bonferroni´s multiple comparison test. (C) HEK 293T cells were transiently transfected with the indicated YFP labeled receptors, arrestin-3 CFP and GRK2. Individual single-cell recordings of agonist-induced alterations in FRET between arrestin-3 and different β2AR mutants were averaged (mean ± S.E.M.; n≥6) and are shown as absolute alterations in FRET. For better visualization mean curves for β2AR 3S or β2AR 2S are displayed + or - S.E.M. of $\Delta(F_{YFP} / F_{CFP})$. ** p < 0.01; * p <

Molecular Pharmacology Fast Forward. Published on November 25, 2014 as DOI: 10.1124/mol.114.095422
This article has not been copyedited and formatted. The final version may differ from this version.



0.5; ANOVA followed by Dunnett´s multiple comparison test. (D) Relative expression levels of β2AR mutants and arrestin-3, as measured by comparing CFP and YFP fluorescence, were not significantly different between the conditions.

*Figure 6. Arrestin-3 mobility determined by dual color FRAP in the continuous presence of agonist*

HEK 293T cells were transiently transfected with either β2AR, β2V2R chimera or $\beta2AR^{SSS}$ tagged N-terminally with YFP and arrestin-3-CFP. Cells were preincubated with a polyclonal anti-YFP antibody for 30 min at 37°C before being stimulated with 10 μM isoprenaline. (A,B) Arrestin-3-CFP and YFP-tagged receptors were photobleached in a small spot at the membrane by high confocal laser intensities and redistribution of both was measured for at least 180 s using low laser intensities. The scale bar represents 1 μm. Mean recovery for arrestin-3 (C) or receptors (D) was calculated (n=17-23), $k_{fast}$ and $k_{slow}$ were fitted to a biphasic exponential equation as described in Methods. Mean recovery and corresponding $t_{0.5}$ values are summarized in Table 1. (E) $k_{slow}$ ± S.E. ***p < 0.001, ANOVA followed by Dunnett´s multiple comparison test. (F) Recovery of YFP-β2AR without anti-YFP pretreatment.

*Figure 7. μ-Patterning for quantification of arr-3 mobility with β2AR and $\beta2AR^{SSS}$ via TIRF microscopy*

HeLa cells transiently expressing Flag-β2AR-CFP, GRK2 and YFP-arr-3 were grown on a μ-biochip coated with anti-Flag antibodies. (A) Accurate alignment of anti-Flag antibodies into unblocked spots leads to enrichment of the bait protein (β2AR) into μ-patterns. Co-localization of the prey protein (arr-3) in anti-Flag antibody-positive regions indicated specific protein-protein interactions. Stimulation with 10 μM isoprenaline significantly increased the basic fluorescent contrast for arr-3. (B) Quantification of β2AR-arr-3 interaction by contrast evaluation. p<0.05, Student´s t-test. (C) Photobleaching experiments on μ-biochips. Individual arrestin-3 patterns were selected for the FRAP experiment. Images show a representative cell with a single bleached spot before and at the indicated time points after photobleaching for β2AR (upper panel) and $\beta2AR^{SSS}$ (lower panel). Scale bars represent 10 μm.(D) Normalized mean recovery curves for arrestin-3 were calculated (n=17 for each condition), $k_{fast}$ and $k_{slow}$ were fitted to a biphasic exponential equation as described in the methods section. (E) $k_{slow}$ ± S.E. ***p<0.001 with Student's t-test.

Molecular Pharmacology Fast Forward. Published on November 25, 2014 as DOI: 10.1124/mol.114.095422
This article has not been copyedited and formatted. The final version may differ from this version.



*Figure 8. Cellular trafficking of arrestin-3 with β2AR, β2AR$^{SSS}$, and β2V2R*

(A) HEK 293T cells were transiently transfected with YFP-labeled β2AR, β2AR$^{SSS}$ or β2V2R, arrestin-3-CFP and GRK2. Cells were stimulated or not for 30 min with 10 μM isoprenaline at 37°C, fixed and imaged by confocal microscopy. The scale bars represent 10 μm. β2AR, β2AR$^{SSS}$ or β2V2R appeared mostly at the plasma membrane under basal conditions whereas arrestin-3 appeared mostly in the cytoplasm. Following isoprenaline treatment internalized receptors were observed as punctate staining on the membrane or in the cytoplasm. Co-localized receptor and arrestin-3 are observed as yellow spots (arrows) when the images are merged. (B) Pearson´s correlation coefficient calculated for colocalization of arrestin-3-CFP and indicated YFP-labeled receptors (mean ± S.E.; n ≥ 7). ***p < 0.001, ANOVA followed by Bonferroni´s multiple comparison test.

*Figure 9. Colocalization of arrestin-3 with EEA1 after β2AR, β2AR$^{SSS}$, and β2V2R stimulation*

(A) Confocal images of HEK 293T cells transiently expressing β2AR, β2AR$^{SSS}$ or β2V2R, arr-3-CFP, GRK2, and mCherry-EEA1. Cells were stimulated or not with 10 μM isoprenaline for 30 min at 37°C, fixed and analyzed for colocalization of arrestin-3 and EEA1. Scale bar represents 10 μm. (B) Pearson´s correlation coefficients calculated for arrestin-3-CFP and mCherry-EEA1 colocalization (n=7-10), mean±S.E. ***p<0.001, ANOVA followed by Bonferroni´s multiple comparison test.

*Figure 10. Agonist-induced receptor internalization and recycling after agonist removal*

(A) HEK 293T cells transiently transfected with β2AR or β2AR$^{SSS}$ were stimulated with 1 μM isoprenaline for 30 min at 37°C. Internalization after 30 min was significantly different between β2AR and β2AR$^{SSS}$; * p< 0.05, Student´s t-test. After agonist removal on ice receptors were allowed to recycle for the indicated time points at 37°C. Receptor surface expression was measured as described under "Experimental procedures". Points represent mean surface receptor recovery ± S.E.M., normalized to the maximum of receptor expression before receptor stimulation. (B) In order to show the kinetics of recycling, the recovery of β2AR or β2ARSSS to the plasma membrane was normalized to the receptor surface

Molecular Pharmacology Fast Forward. Published on November 25, 2014 as DOI: 10.1124/mol.114.095422
This article has not been copyedited and formatted. The final version may differ from this version.



expression before ligand treatment as a maximum and to the internalization after 30 min of ligand stimulation as a minimum.

Molecular Pharmacology Fast Forward. Published on November 25, 2014 as DOI: 10.1124/mol.114.095422
This article has not been copyedited and formatted. The final version may differ from this version.



**Table 1**

*Kinetic constants of FRET and FRAP experiments for arrestin-3 interaction with various receptors*

Summary of the kinetic parameters measured in the various fluorescence experiments. For FRET assays (upper panel), $k_{on}$, $k_{off}$, and $t_{0.5}$ of arrestin association and dissociation as well as the portion of arrestin dissociation were obtained by monoexponential curve fitting as described in the methods section. Association rates of arrestin without GRK2 overexpression could not be determined by curve fitting (n.a.: not applicable) as the plateau was not reached during the timescale of the experiment (upper panel). For the FRAP experiments by confocal (middle panel) and TIRF microscopy (lower panel), the kinetic parameters $k_{on\ fast}$ and $k_{on\ slow}$ of FRAP experiments were obtained by bi-exponential curve fitting. $t_{0.5}$ values were obtained by calculating ln(2)/k.

Molecular Pharmacology Fast Forward. Published on November 25, 2014 as DOI: 10.1124/mol.114.095422
This article has not been copyedited and formatted. The final version may differ from this version.



| **FRET** | $k_{on}$ ± S.E.M. ($s^{-1}$) | $k_{off}$ ± S.E.M. ($s^{-1}$) | $t_{0.5\ on}$ (s) | $t._{0.5\ off}$ (s) | Portion of arr3 dissociation ± S.E.M. (%) |
|---|---|---|---|---|---|
| β2AR (+GRK2) | 0.040 ± 0.004 | 0.025 ± 0.001 | 17.3 | 27.7 | 69.1 ± 2.1 |
| β2AR AAA (+GRK2) | 0.017 ± 0.002 | 0.026 ± 0.002 | 40.8 | 26.7 | 65.3 ± 3.2 |
| β2AR SSS (+GRK2) | 0.061 ± 0.008 | 0.011 ± 0.0007 | 11.4 | 63.0 | 36.1 ± 3.1 |
| β2V2R (+GRK2) | 0.026 ± 0.004 | 0.020 ± 0.002 | 26.7 | 34.7 | 27.4 ± 4.9 |
| β2AR | n.a. | 0.026 ± 0.002 | n.a. | 26.7 | 59.1 ± 5.1 |
| $\beta2AR^{SSS}$ | n.a. | 0.019 ± 0.002 | n.a. | 36.5 | 41.7 ± 5.6 |

| **FRAP Confocal** | Arr3 recovery ± S.E.M (%) | $k_{fast}$ ± S.E.M. ($s^{-1}$) | $k_{slow}$ ± S.E.M. ($s^{-1}$) | fast half life (s) | slow half life (s) |
|---|---|---|---|---|---|
| β2AR | 54.6 ± 2.6 | 0.185 ± 0.015 | 0.019 ± 0.001 | 3.8 | 36.5 |
| $\beta2AR^{SSS}$ | 51.3 ± 5.1 | 0.085 ± 0.017 | 0.012 ± 0.001 | 8.2 | 57.8 |
| β2V2R | 21.3 ± 2.7 | 0.143 ± 0.038 | 0.006 ± 0.001 | 4.9 | 115.5 |

| **FRAP TIRF** | Arr3 recovery ± S.E.M. (%) | $k_{fast}$ ± S.E.M. ($s^{-1}$) | $k_{slow}$ ± S.E.M. ($s^{-1}$) | fast half life (s) | slow half life (s) |
|---|---|---|---|---|---|
| β2AR | 70.3 ± 1.5 | 0.187 ± 0.023 | 0.016 ± 0.003 | 3.70 | 42.13 |
| $\beta2AR^{SSS}$ | 75.2 ± 3.9 | 0.270 ± 0.170 | 0.004 ± 0.0003 | 2.56 | 152 |

Molecular Pharmacology Fast Forward. Published on November 25, 2014 as DOI: 10.1124/mol.114.095422
This article has not been copyedited and formatted. The final version may differ from this version.



Figure 1

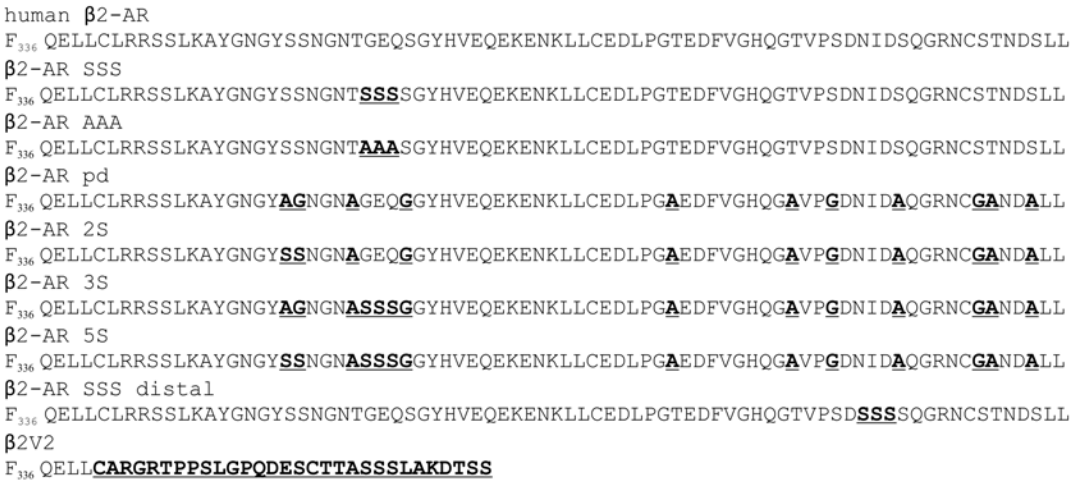

Figure 2

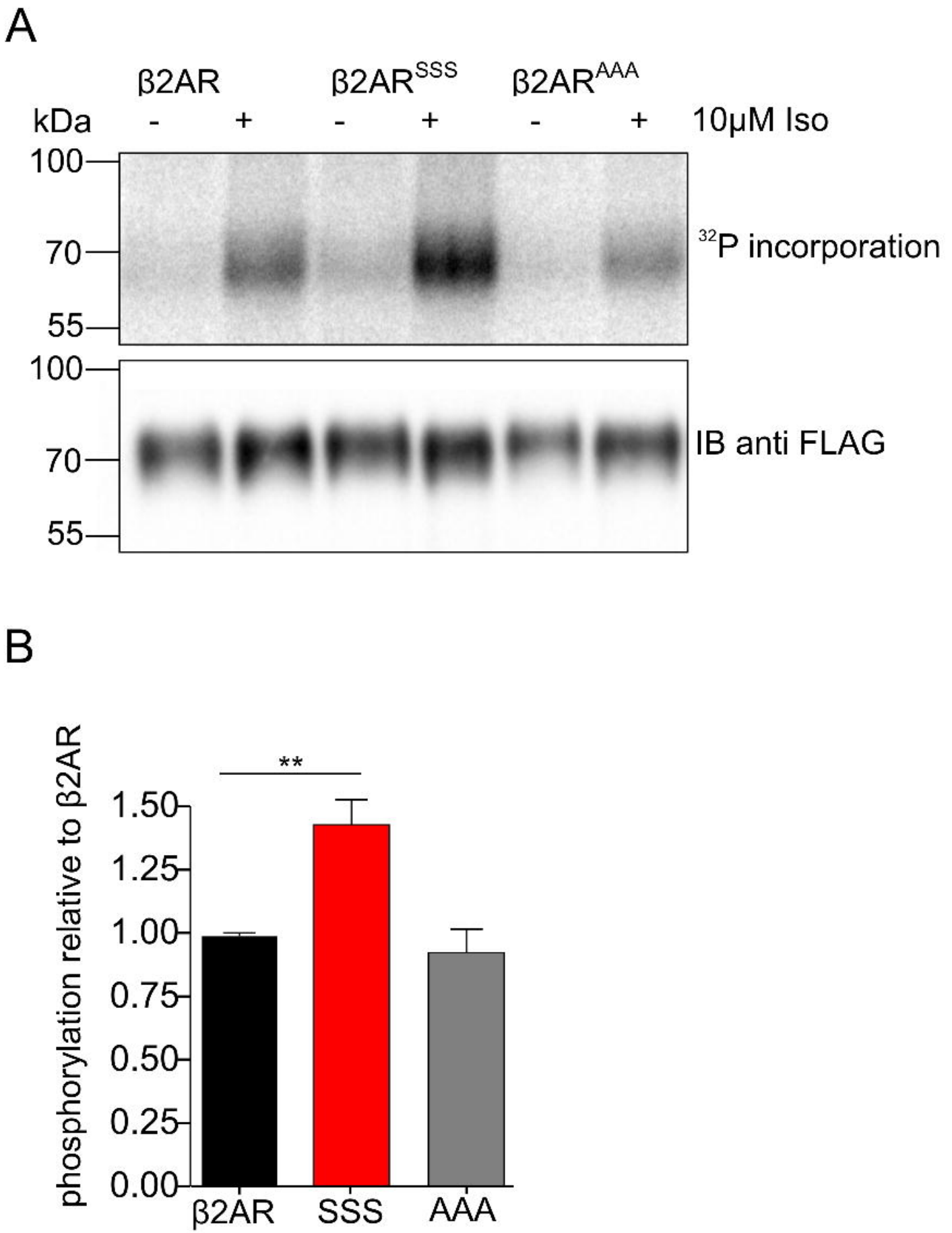
A
β2AR
β2AR^SSS
β2AR^AAA
kDa
-
+
-
+
-
+
10μM Iso
100
70
55
32P incorporation
100
70
55
IB anti FLAG
B
phosphorylation relative to β2AR
**
1.50
1.25
1.00
0.75
0.50
0.25
0.00
β2AR
SSS
AAA

Figure 3

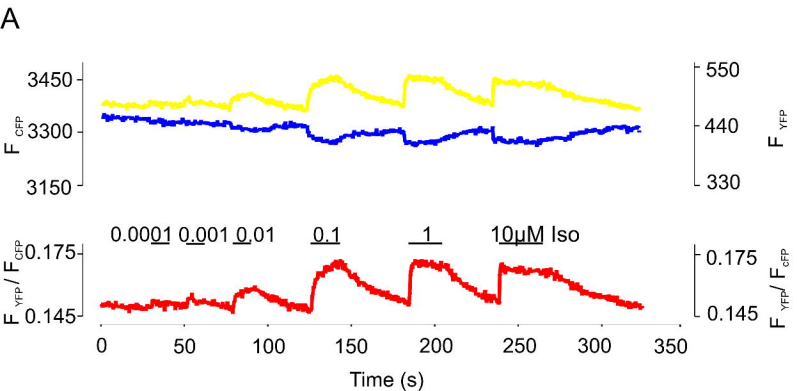
A
3450
3300
3150
F CFP
550
440
330
F YFP
0.0001 0.001 0.01 0.1 1 10μM Iso
0.175
0.145
F YFP / F CFP
0.175
0.145
F YFP / F CFP
0
50
100
150
200
250
300
350
Time (s)

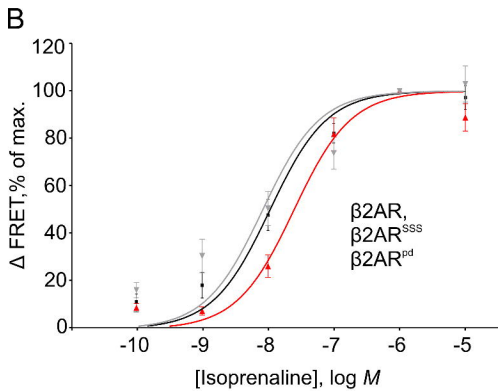
B
120
100
80
60
40
20
0
Δ FRET,% of max.
β2AR,
β2AR^sss
β2AR^pd
-10
-9
-8
-7
-6
-5
[Isoprenaline], log M

Figure 4

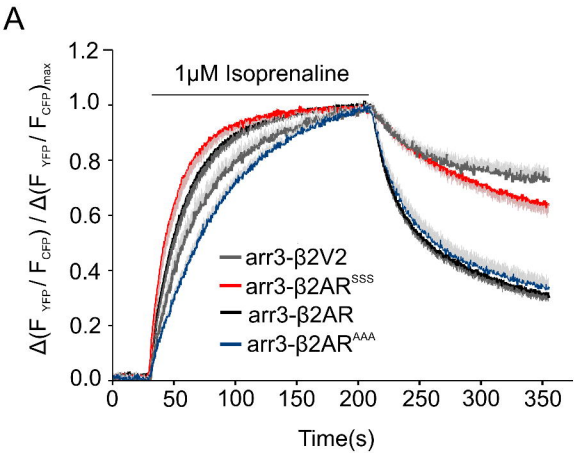
A
1μM Isoprenaline
arr3-β2V2
arr3-β2AR^SSS
arr3-β2AR
arr3-β2AR^AAA
Δ(F YFP / F CFP) / Δ(F YFP / F CFP)max
Time(s)

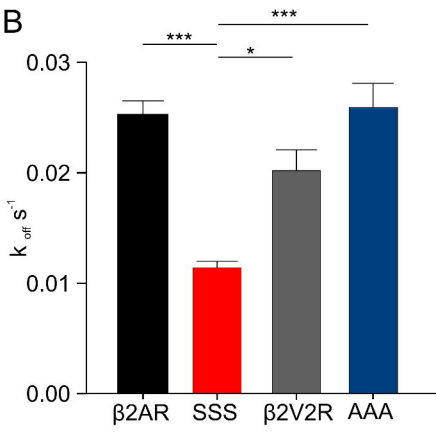
B
***
***
*
k off s-1
β2AR
SSS
β2V2R
AAA

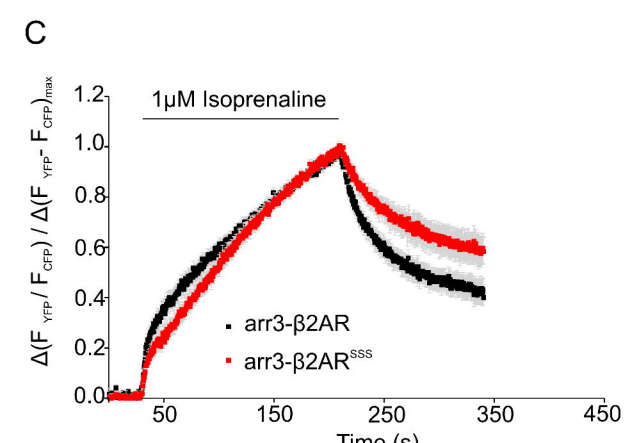
C
1μM Isoprenaline
arr3-β2AR
arr3-β2AR^SSS
Δ(F YFP / F CFP) / Δ(F YFP- F CFP)max
Time (s)

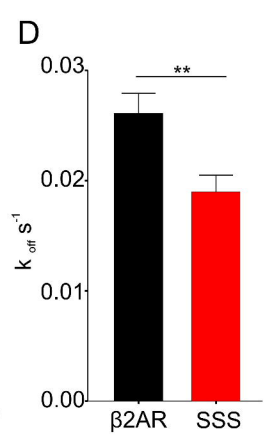
D
**
k off s-1
β2AR
SSS

Figure 5

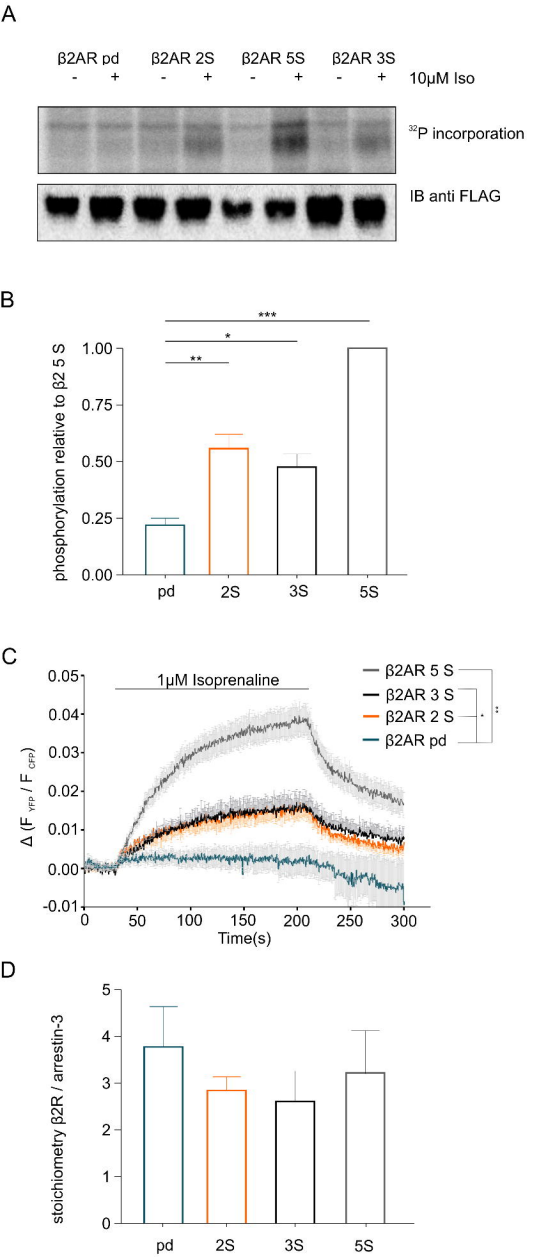
A
β2AR pd
β2AR 2S
β2AR 5S
β2AR 3S
- + - + - + - +
10μM Iso
32P incorporation
IB anti FLAG
B
phosphorylation relative to β2 5 S
1.00
0.75
0.50
0.25
0.00
***
*
**
pd
2S
3S
5S
C
1μM Isoprenaline
β2AR 5 S
β2AR 3 S
β2AR 2 S
β2AR pd
**
*
Δ (FYFP / FCFP)
0.05
0.04
0.03
0.02
0.01
0.00
-0.01
0
50
100
150
200
250
300
Time(s)
D
stoichiometry β2R / arrestin-3
5
4
3
2
1
0
pd
2S
3S
5S

Figure 6

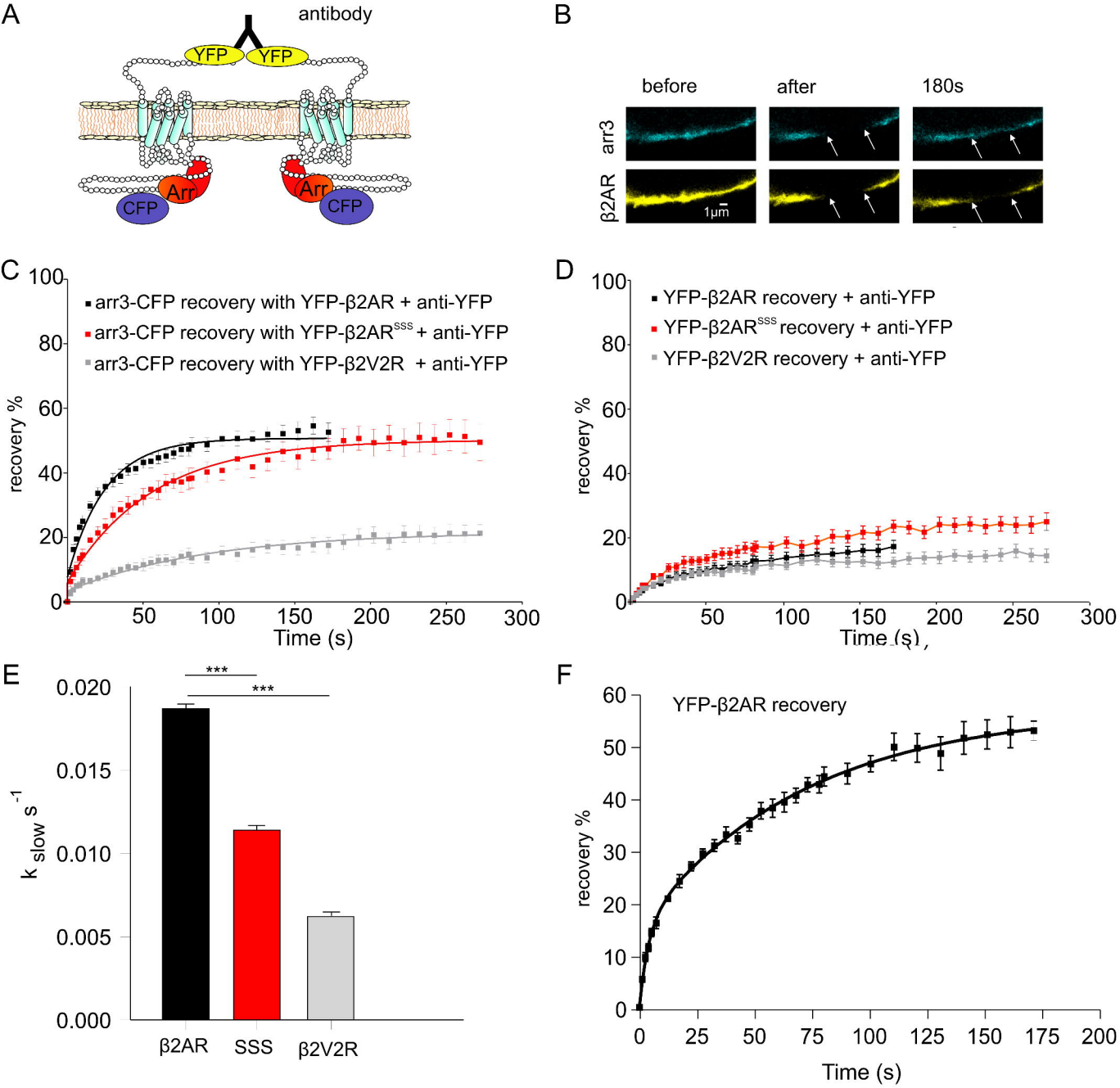
A
antibody
YFP
YFP
Arr
Arr
CFP
CFP
B
before
after
180s
arr3
β2AR
1μm
C
arr3-CFP recovery with YFP-β2AR + anti-YFP
arr3-CFP recovery with YFP-β2AR^sss + anti-YFP
arr3-CFP recovery with YFP-β2V2R + anti-YFP
recovery %
Time (s)
D
YFP-β2AR recovery + anti-YFP
YFP-β2AR^sss recovery + anti-YFP
YFP-β2V2R recovery + anti-YFP
recovery %
Time (s)
E
***
***
k slow s^-1
β2AR
SSS
β2V2R
F
YFP-β2AR recovery
recovery %
Time (s)

Figure 7

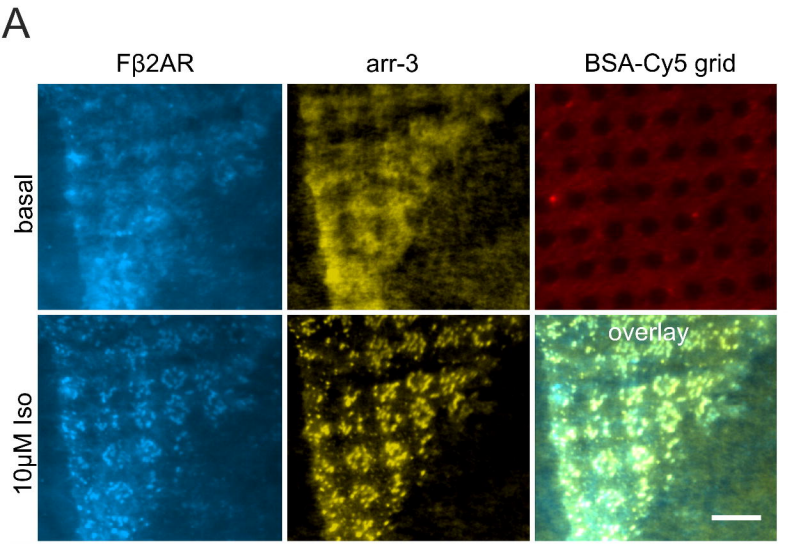
A
Fβ2AR
arr-3
BSA-Cy5 grid
basal
10μM Iso
overlay

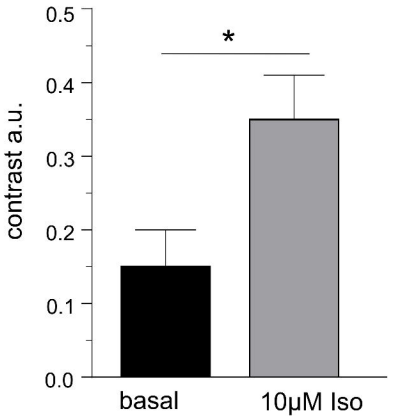
B
contrast a.u.
0.5
0.4
0.3
0.2
0.1
0.0
*
basal
10μM Iso

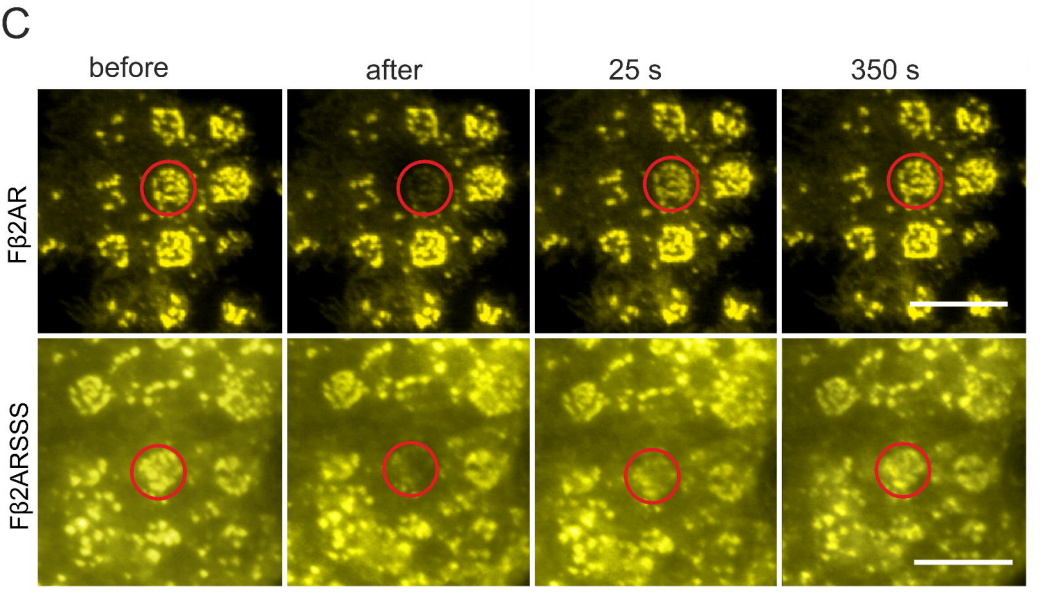
C
before
after
25 s
350 s
Fβ2AR
Fβ2ARSSS

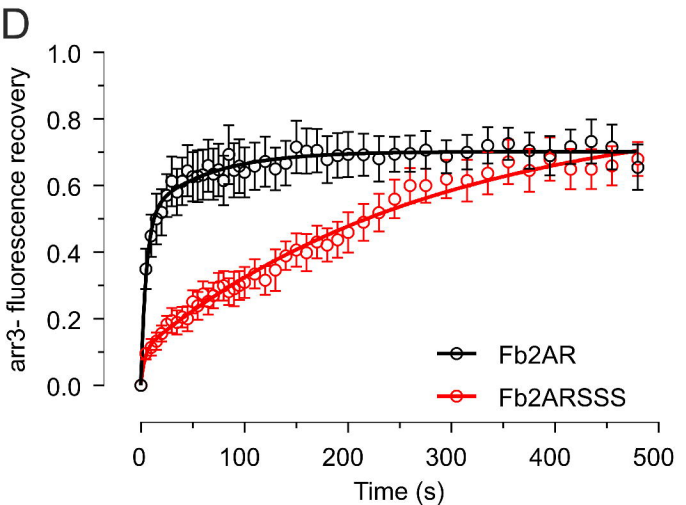
D
arr3- fluorescence recovery
1.0
0.8
0.6
0.4
0.2
0.0
Fb2AR
Fb2ARSSS
0
100
200
300
400
500
Time (s)

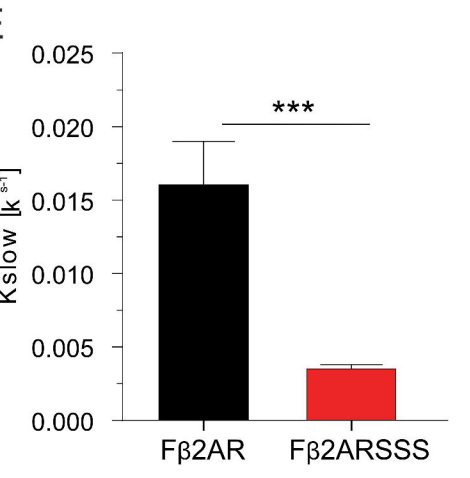
E
Kslow [k s-1]
0.025
0.020
0.015
0.010
0.005
0.000
***
Fβ2AR
Fβ2ARSSS

Figure 8

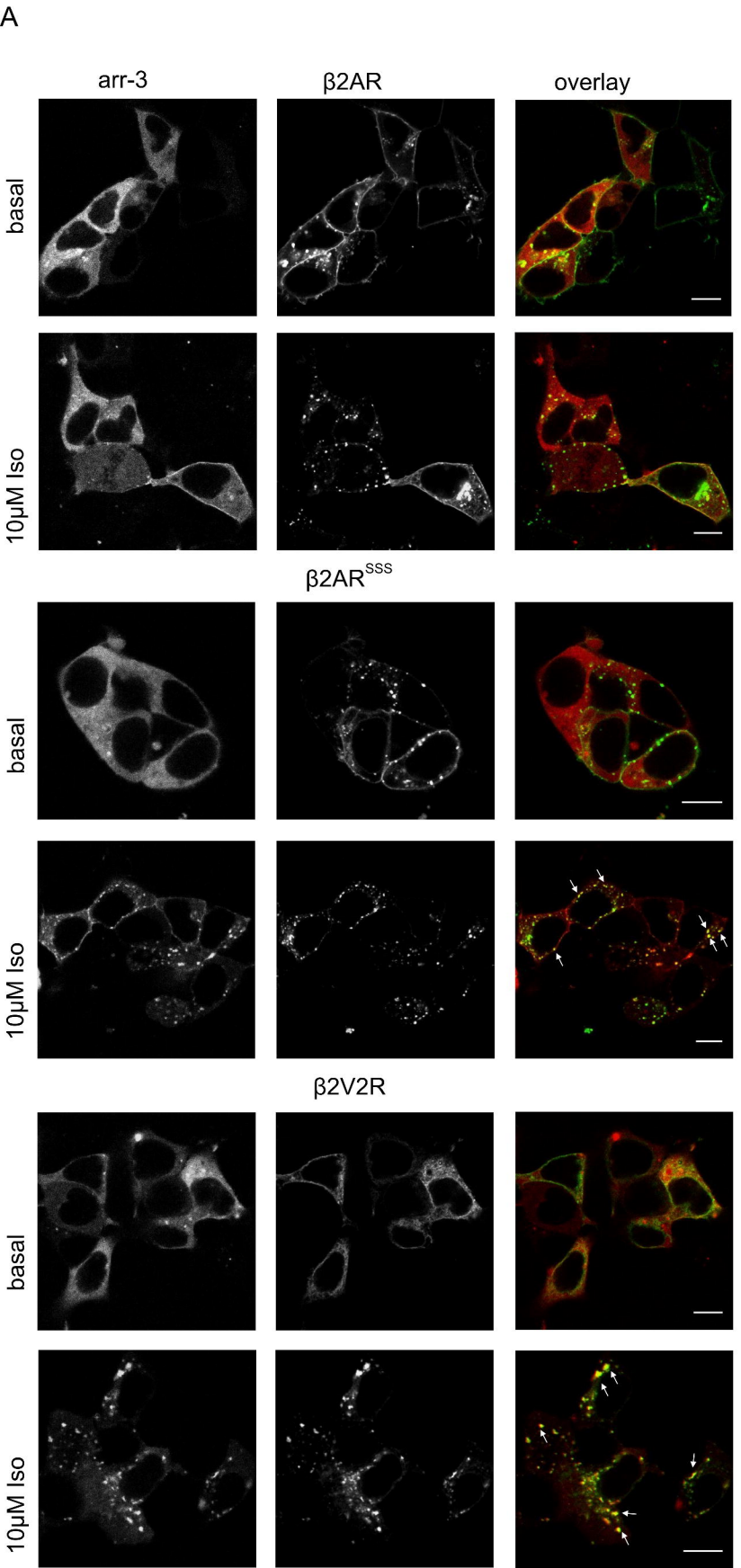
A
arr-3
β2AR
overlay
basal
10μM Iso
β2AR^SSS
basal
10μM Iso
β2V2R
basal
10μM Iso

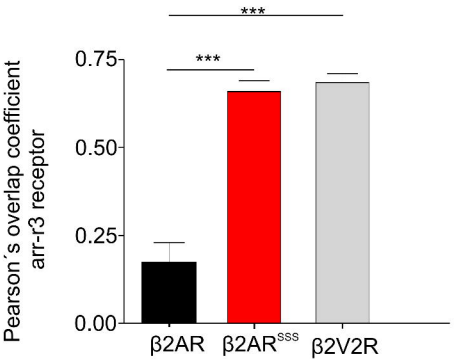
B
***
***
Pearson´s overlap coefficient arr-r3 receptor
0.75
0.50
0.25
0.00
β2AR
β2AR^SSS
β2V2R

Figure 9

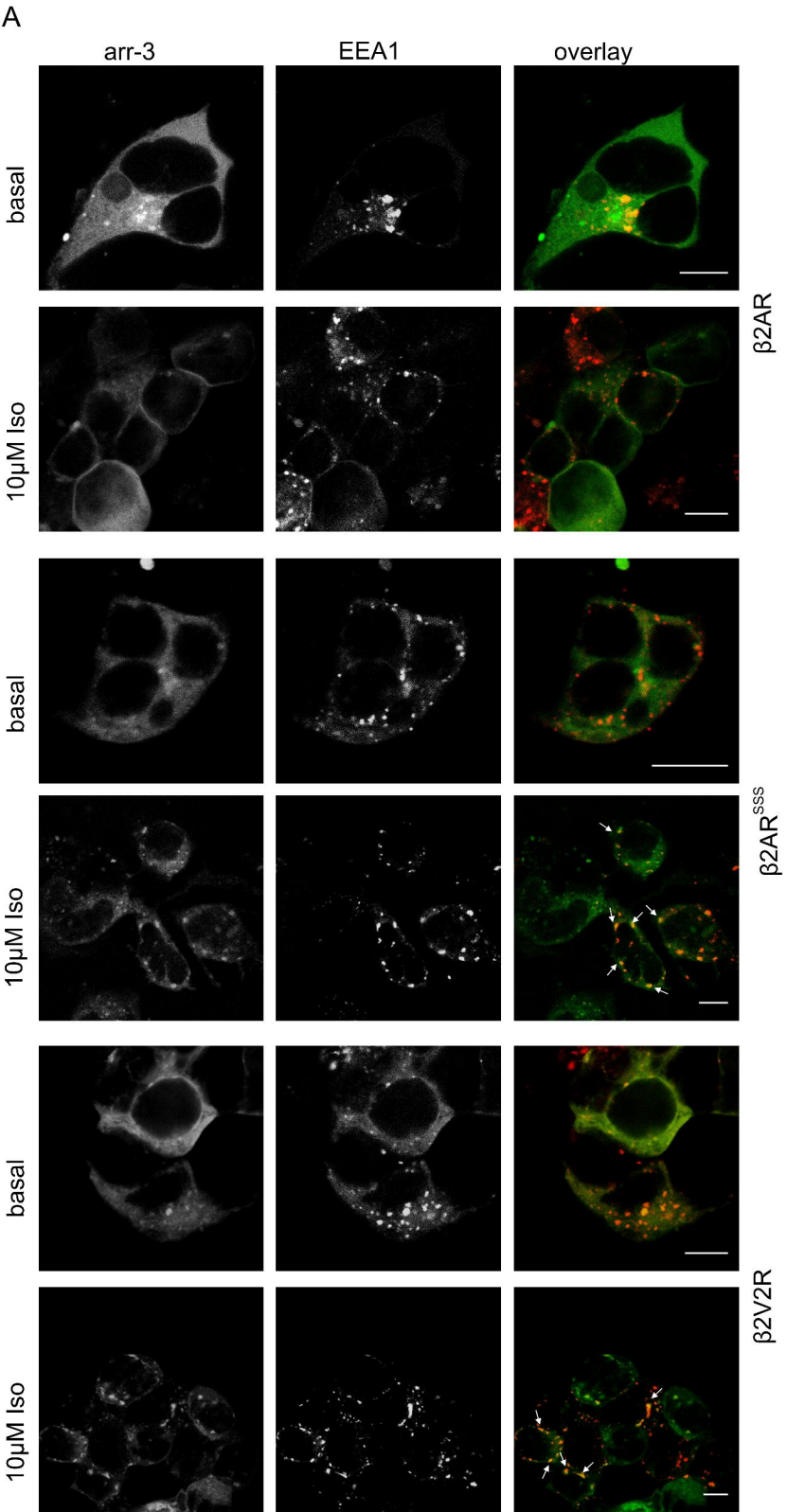
A
arr-3
EEA1
overlay
basal
10µM Iso
β2AR
basal
10µM Iso
β2AR^SSS
basal
10µM Iso
β2V2R

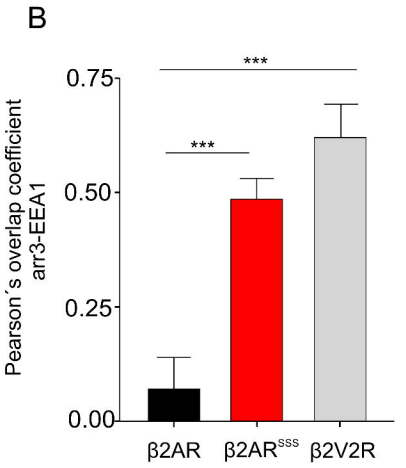
B
Pearson´s overlap coefficient
arr3-EEA1
0.75
0.50
0.25
0.00
***
***
β2AR
β2AR^SSS
β2V2R

Figure 10

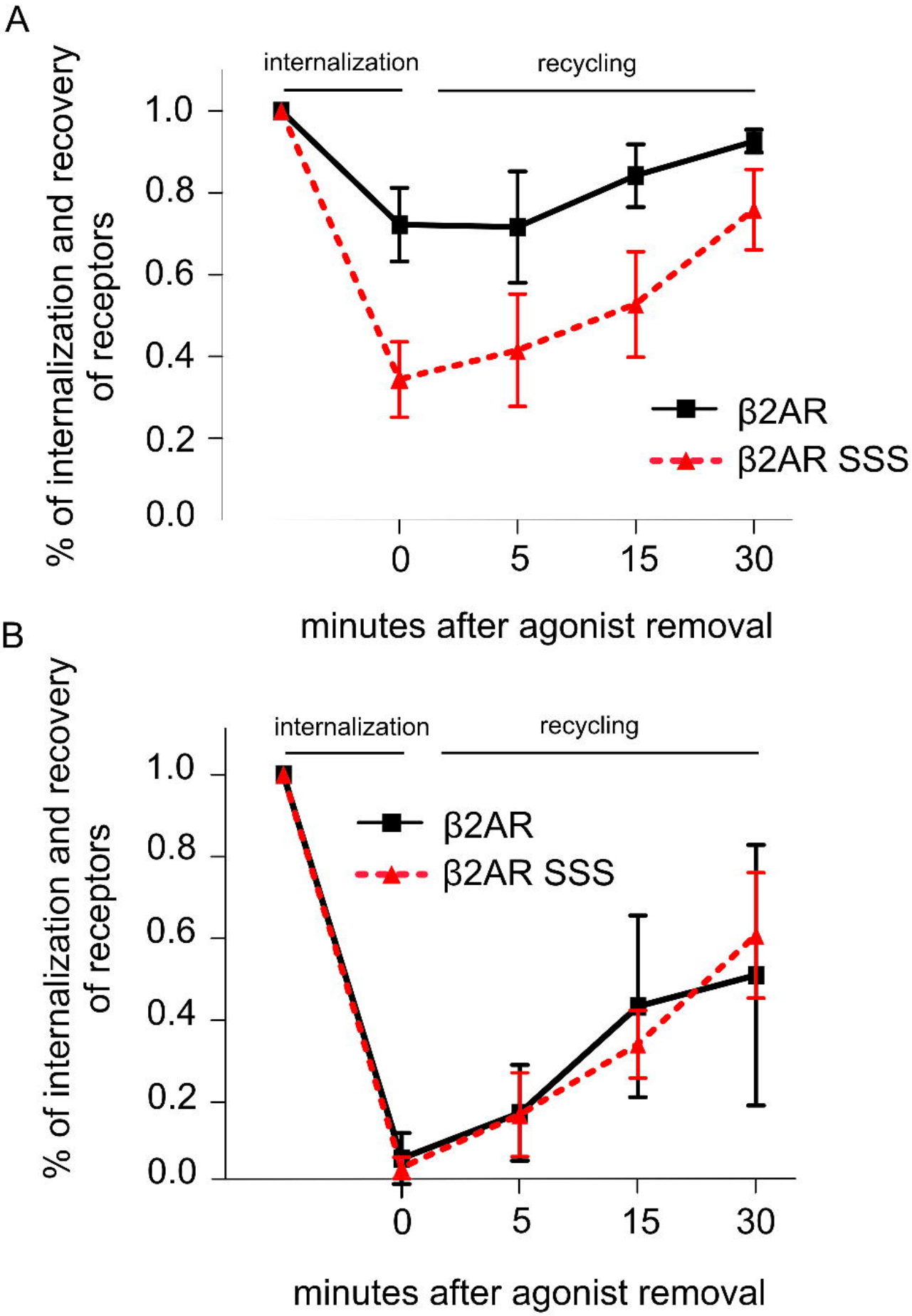
A
internalization
recycling
1.0
0.8
0.6
0.4
0.2
0.0
% of internalization and recovery of receptors
β2AR
β2AR SSS
0
5
15
30
minutes after agonist removal
B
internalization
recycling
1.0
0.8
0.6
0.4
0.2
0.0
% of internalization and recovery of receptors
β2AR
β2AR SSS
0
5
15
30
minutes after agonist removal